

Mass Spectrometric Investigations of the Atmospheres of Giant Planets

Peter Wurz

Physics Institute, University of Bern
Sidlerstrasse 5, 3012 Bern, Switzerland

Science Objectives for Giant Planet's Atmospheres

Scientific Objective ¹	Measurement Objective	Measurement Requirements
Constrain our models and understanding of Ice Giant's formation and subsequent evolution in situ measurement of elemental constituents and isotopic abundances for comparison with elemental compositions observed in the Sun, meteorites, and other planetary atmospheres	Determine fractional abundance of helium relative to H ₂ Determine atmospheric abundance ratios of C, H, O, N, and noble gases	H ₂ /He ratio to an accuracy of 1% C/H, N/H, O/H to a precision of $\pm 10\%$ or better Ne/He, Ar/He, Kr/He, Xe/He to a precision of $\pm 30\%$ or better
	Determine isotopic ratios of C, H, O, N, and noble gases	¹³ C/ ¹² C, ¹⁸ O/ ¹⁶ O to $\pm 1\%$ or better D/H, ¹⁵ N/ ¹⁴ N in major molecular species to $\pm 1\%$ to 5% Isotopic ratios of He, Ne, Ar, Kr, Xe to $\pm 5\%$ to $\pm 10\%$ or better
Determine the strength of vertical mixing in Ice Giant's atmosphere	Determine the vertical abundance profiles of CH ₄ , CO, PH ₃ , H ₂ S, NH ₃ , and others	Measure abundances with uncertainty of a factor of 2 or less
Constrain models of cloud formation and structure	Determine abundances of condensable species below cloud base	e.g., H ₂ O, H ₂ S, and NH ₃ to a factor of 2 or better

O. Mousis, et al., *Scientific rationale for Uranus and Neptune in situ explorations*, Plan. Sp. Sc. 155 (2018), 12-40

Science Objectives for Giant Planet's Atmospheres

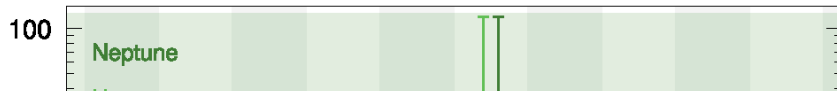


Table 2

Ratios to protosolar values in the upper tropospheres of Jupiter, Saturn, Uranus and Neptune.

Table 1

Elemental abundances in Jupiter, Saturn, Uranus and Neptune, as derived from upper tropospheric composition.

Elements	Jupiter	Saturn	Uranus	Neptune
He/H ^a	$(7.85 \pm 0.16) \times 10^{-2}$	$(6.75 \pm 1.25) \times 10^{-2}$	$(8.88 \pm 2.00) \times 10^{-2}$	$(8.96 \pm 1.46) \times 10^{-2}$
Ne/H ^b	$(1.240 \pm 0.014) \times 10^{-5}$	–	–	–
Ar/H ^b	$(9.10 \pm 1.80) \times 10^{-6}$	–	–	–
Kr/H ^b	$(4.65 \pm 0.85) \times 10^{-9}$	–	–	–
Xe/H ^b	$(4.45 \pm 0.85) \times 10^{-10}$	–	–	–
C/H ^c	$(1.19 \pm 0.29) \times 10^{-3}$	$(2.65 \pm 0.10) \times 10^{-3}$	$(0.6\text{--}3.2) \times 10^{-2}$	$(0.6\text{--}3.2) \times 10^{-2}$
N/H ^d	$(3.32 \pm 1.27) \times 10^{-4}$	$(0.50\text{--}2.85) \times 10^{-4}$	–	–
O/H ^e	$(2.45 \pm 0.80) \times 10^{-4}$	–	–	–
S/H ^f	$(4.45 \pm 1.05) \times 10^{-5}$	–	–	–
P/H ^g	$(1.08 \pm 0.06) \times 10^{-6}$	$(3.64 \pm 0.24) \times 10^{-6}$	–	–

^a von Zahn et al. (1998) and Niemann et al. (1998) for Jupiter, Conrath and Gautier (2000) and Atreya et al. (2016) for Saturn, Conrath et al. (1987) for Uranus and Burgdorf et al. (2003) for Neptune. We only consider the higher value of the uncertainty on He in the case of Neptune.

^b Mahaffy et al. (2000) for Jupiter.

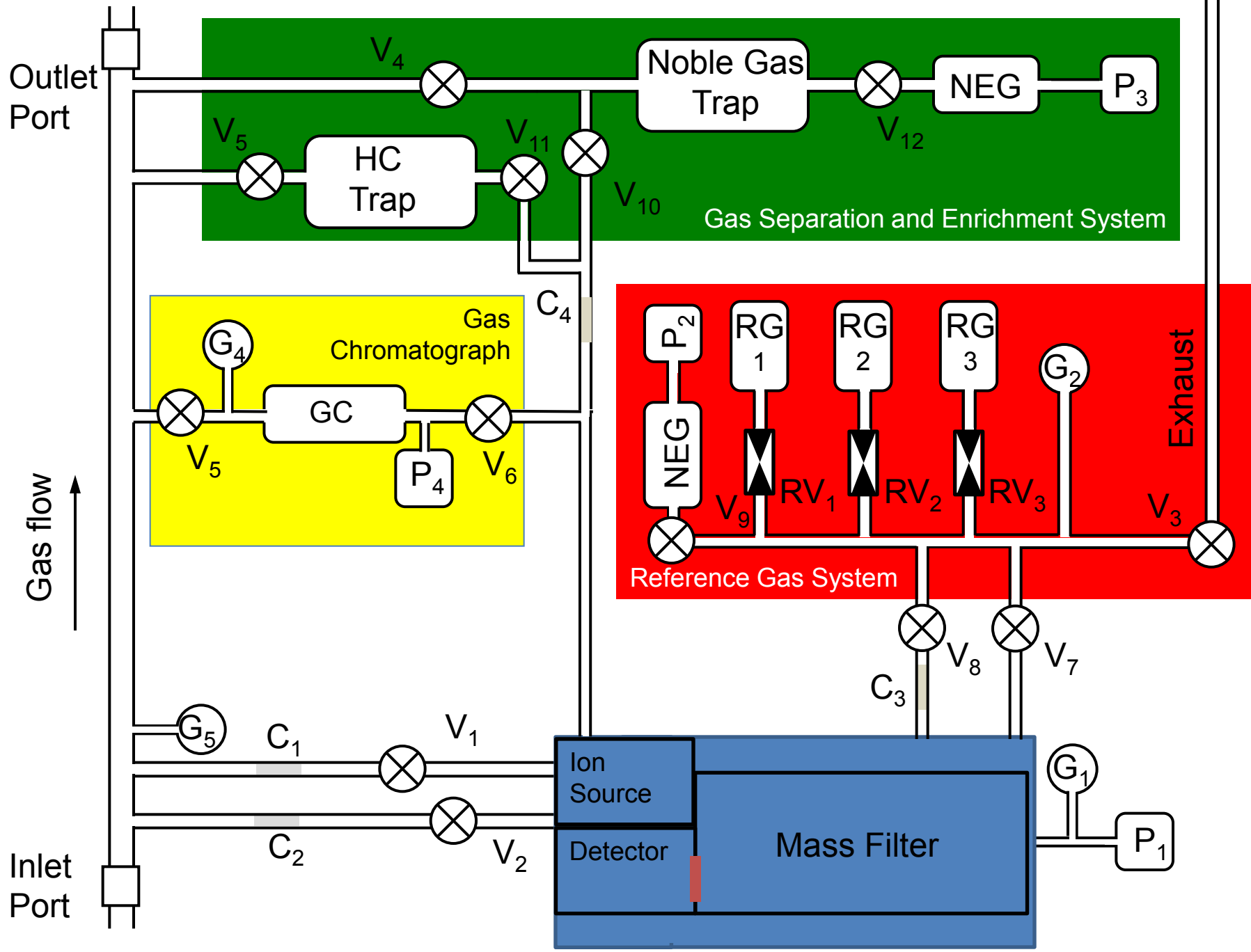
^c Wong et al. (2004) for Jupiter, Fletcher et al. (2009a) for Saturn, Lindal et al. (1987), Baines et al. (1995), Karkoschka and Tomasko (2009), and Sromovsky et al. (2014) for Uranus, Lindal et al. (1990), Baines et al. (1995), and Karkoschka (2011) for Neptune.

^d Wong et al. (2004) for Jupiter, Fletcher et al. (2011) for Saturn (our N/H range is derived from the observed range of 90–500 ppm of NH₃).

^e Wong et al. (2004) for Jupiter (probably a lower limit, not representative of the bulk O/H). de Graauw et al. (1997) has detected H₂O at 5 μm with ISO in Saturn, but the measurement at 1–3 bars is not representative of the bulk O/H.

^f Wong et al. (2004) for Jupiter.

^g Fletcher et al. (2009b) for Jupiter and Saturn.



Top-level Requirements

- ❖ Mass range
 - 1 – 300 u
- ❖ Sufficient mass resolution
 - $m / \Delta m \approx 500$
- ❖ Sufficient sensitivity
 - 10 decades dynamic range, plus isotopes
 - Measurement time 10 – 90 minutes (descent time)
- ❖ Limit complexity
 - Accommodation in the atmospheric probe
- ❖ Limit instrument resources
 - Power, volume, mass

Galileo Probe Mass Spectrometer Experiment

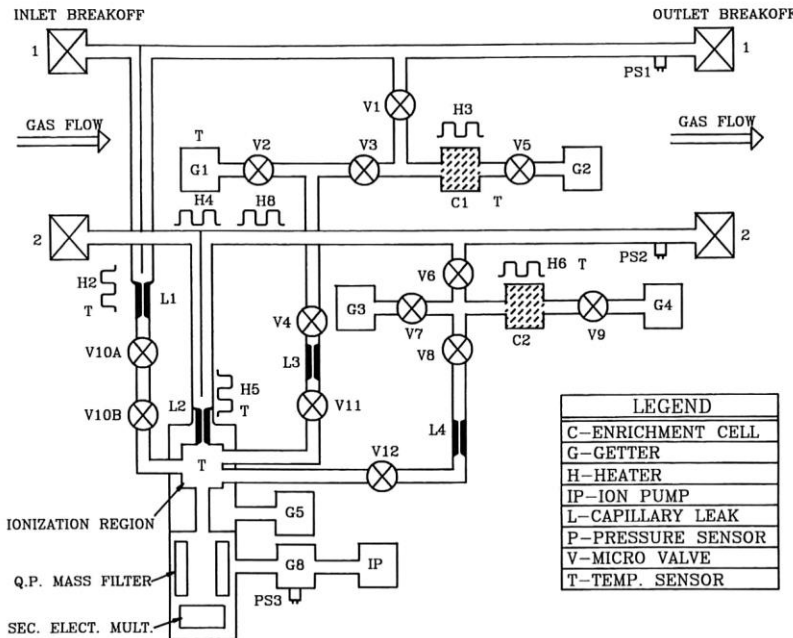


Fig. 1. Schematic of the gas inlet system and connection to the mass spectrometer sensor. Two parallel gas inlet/outlet systems are employed to provide gas samples to the direct leaks, L1 and L2, and to the two sample enrichment systems centered around C1 and C2.

H.B. Niemann, D.N. Harbold, S.K. Atreya, G.R. Cargnan, D.M. Hunten, T.C. Owen, Galileo Probe Mass spectrometer Experiment, Sp. Sci. Rev. 60 (1992) 111–142.

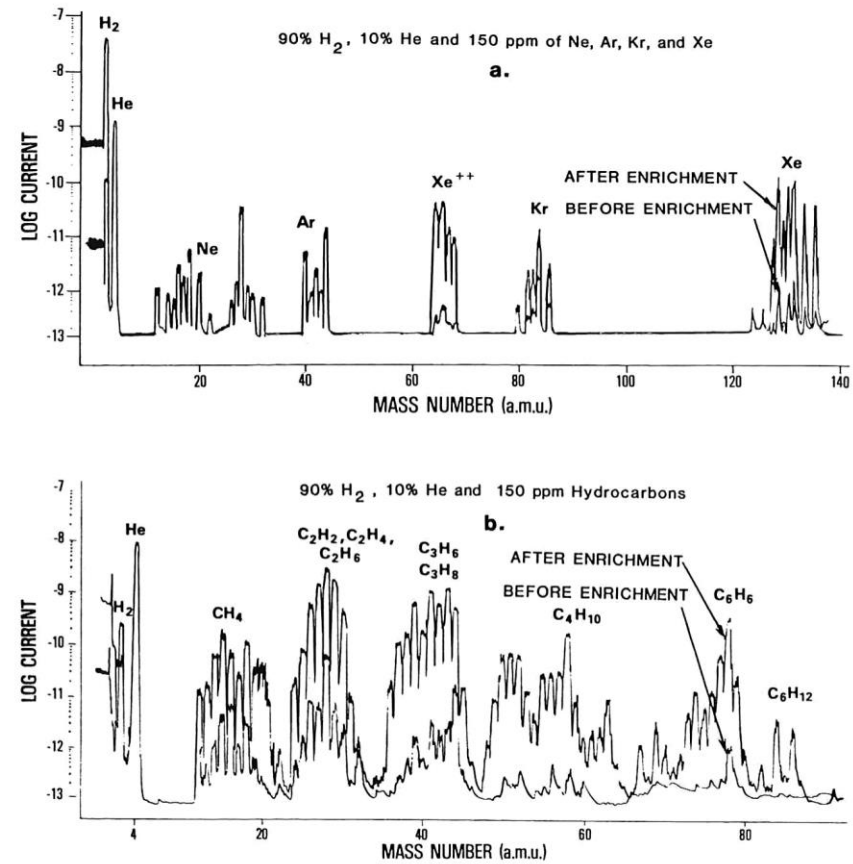


Fig. 2. Mass spectra showing enrichment obtained when gas processing is used to remove the major constituent H₂ from a 90% H₂ and 10% He mixture containing constituents each of 150 ppmv. (a) Rare gas enrichment. Note the substantial enrichment of Xe obtained. Expected Xe ratios are marginally measurable by direct analysis. (b) Hydrocarbon enrichment. There is a substantial enrichment of the C₃–C₄ hydrocarbons with a somewhat less enrichment for methane. For illustration the spectra were recorded analog with laboratory recording equipment.

The Gas Chromatograph Mass Spectrometer for the Huygens Probe

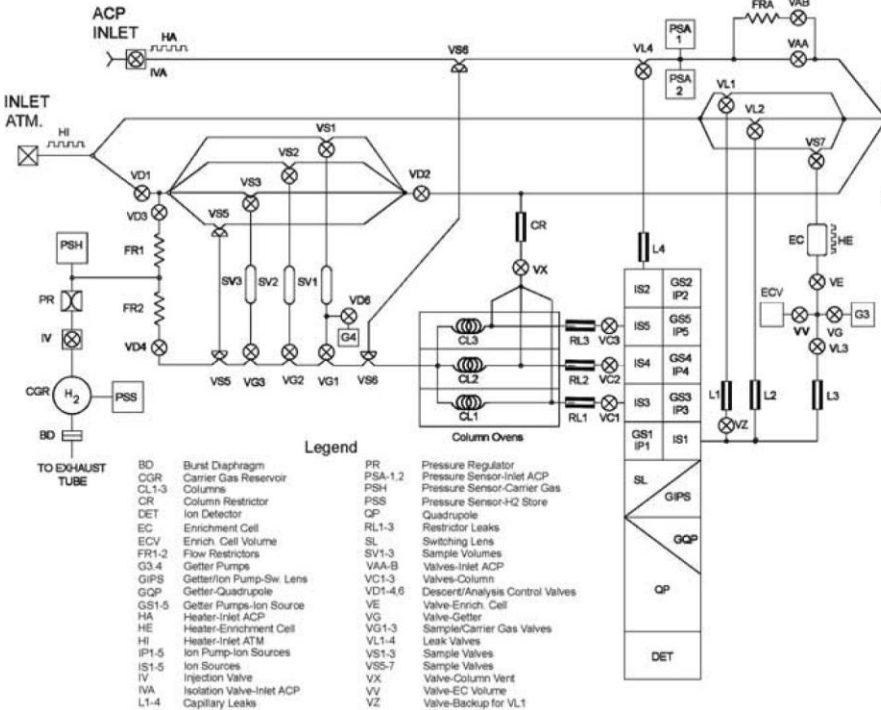


Figure 3. Schematic of the Gas Chromatograph Mass Spectrometer. Details of the Aerosol Collector and Pyrolyser are shown in an accompanying paper in this volume.

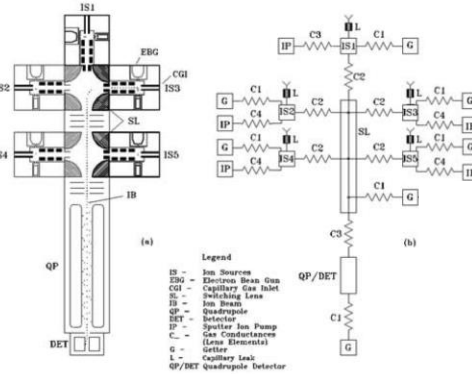


Figure 5. Illustrations of ion source configuration and schematic of the differential vacuum pumping system.

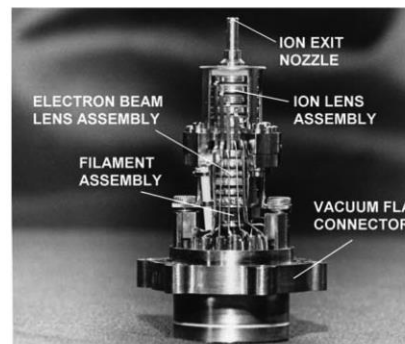


Figure 6. An ion source showing the electron and ion focus. The overall height is 63 mm.

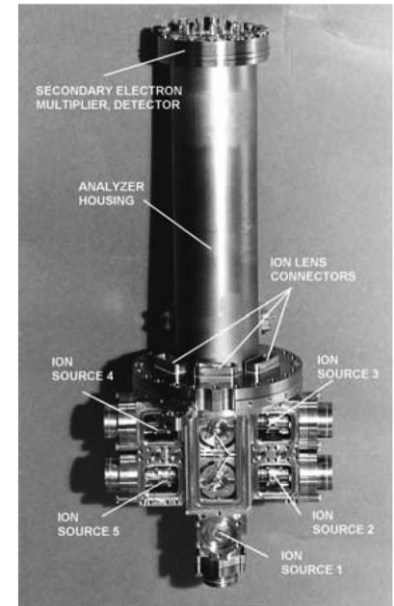
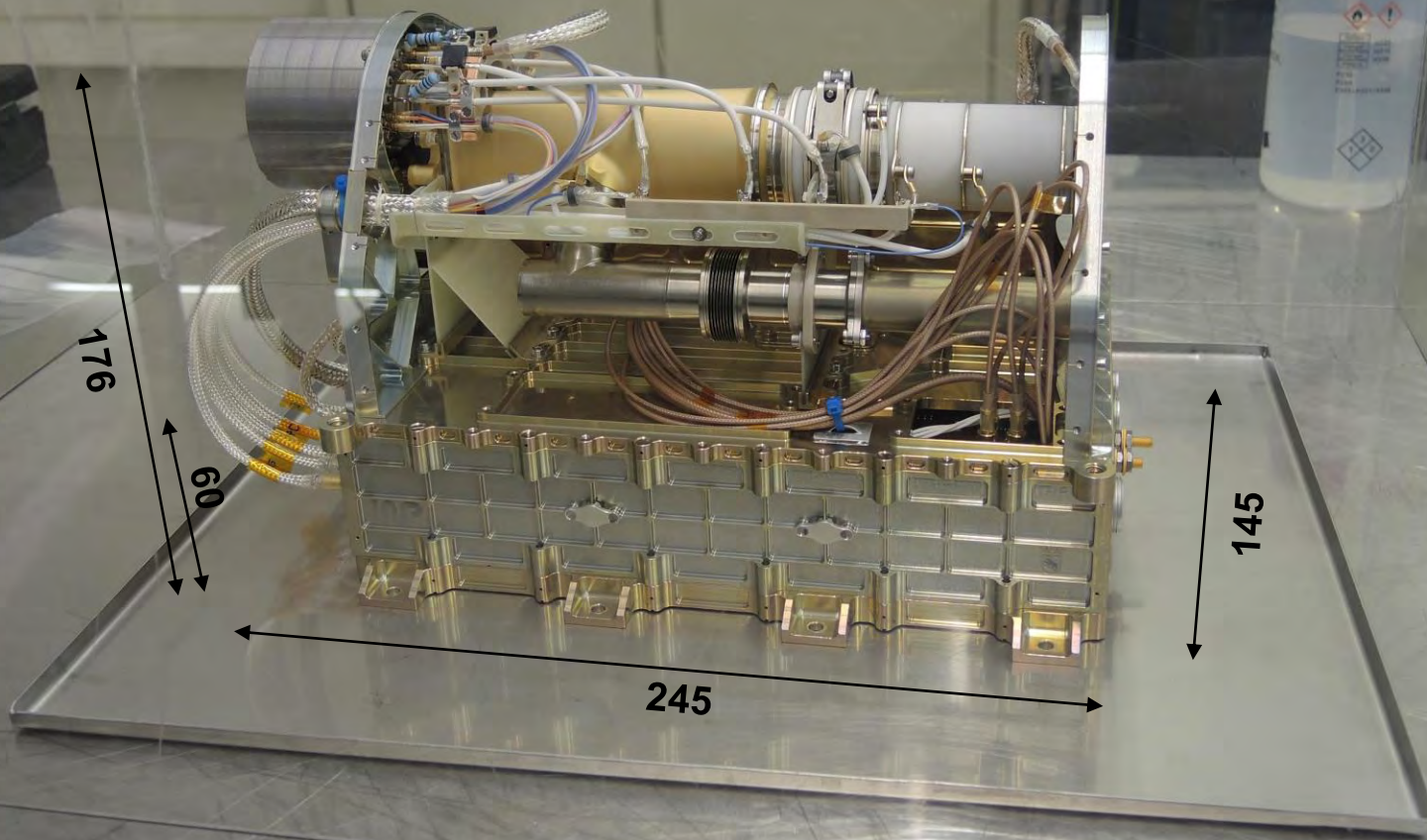


Figure 7. The ion source system, showing the individual ion sources and the switching lenses in the partially assembled ion source housing before installation of the getter housings and the gas inlet manifolds. The overall length is 357 mm.

NGMS / Luna-Resurs GC-MS complex



Mass: 3.5 kg
Power: 19 W

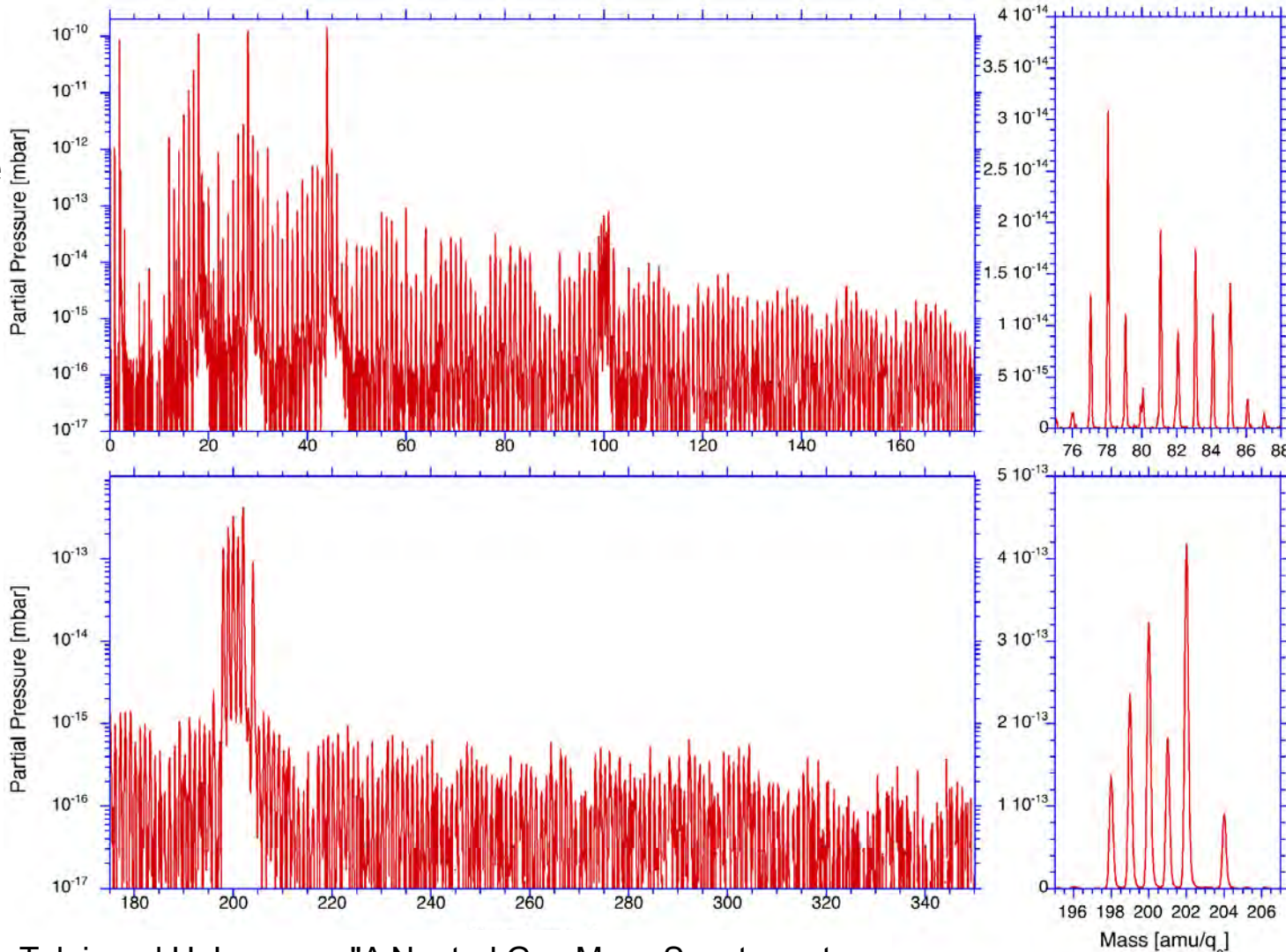
Neutral Gas Mass Spectrometer Luna-Resurs / Luna-Glob

u^b

b
UNIVERSITÄT
BERN

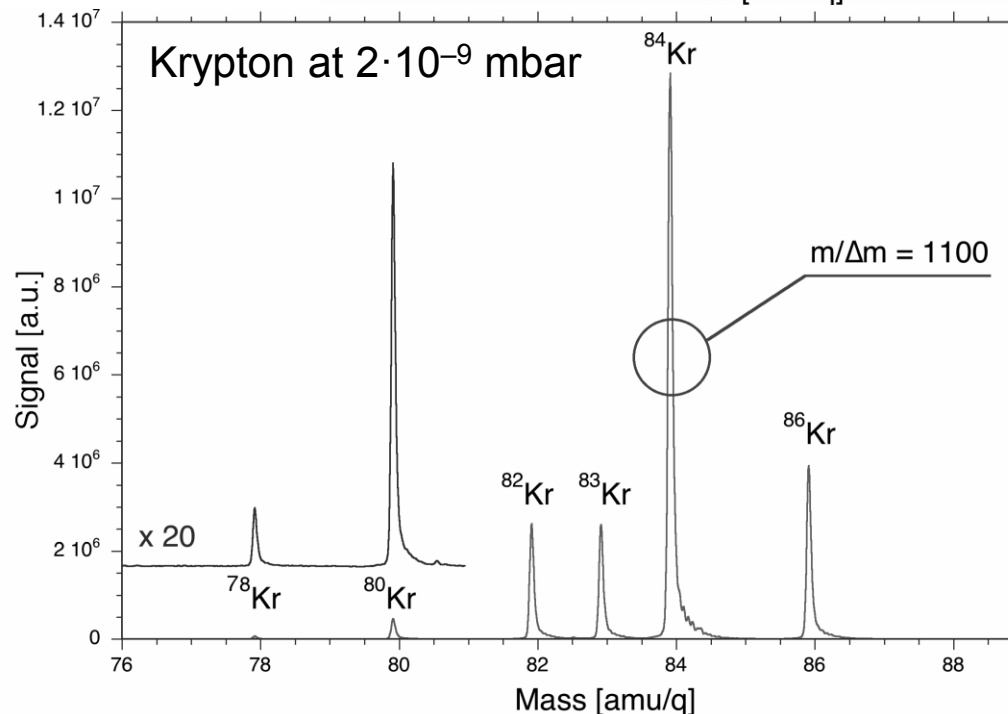
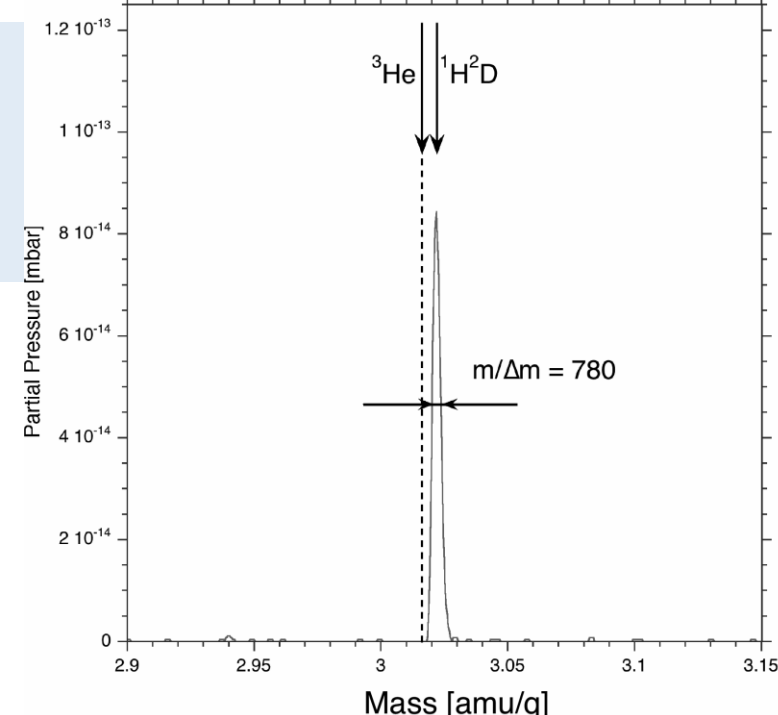
Mass range

- ❖ 1 – 300 amu (low mass range mode)
- ❖ Can be increased in flight by command, if necessary, to 1000 amu (high mass range mode).
- ❖ Mass range is only limited by memory for accumulation



Mass Resolution

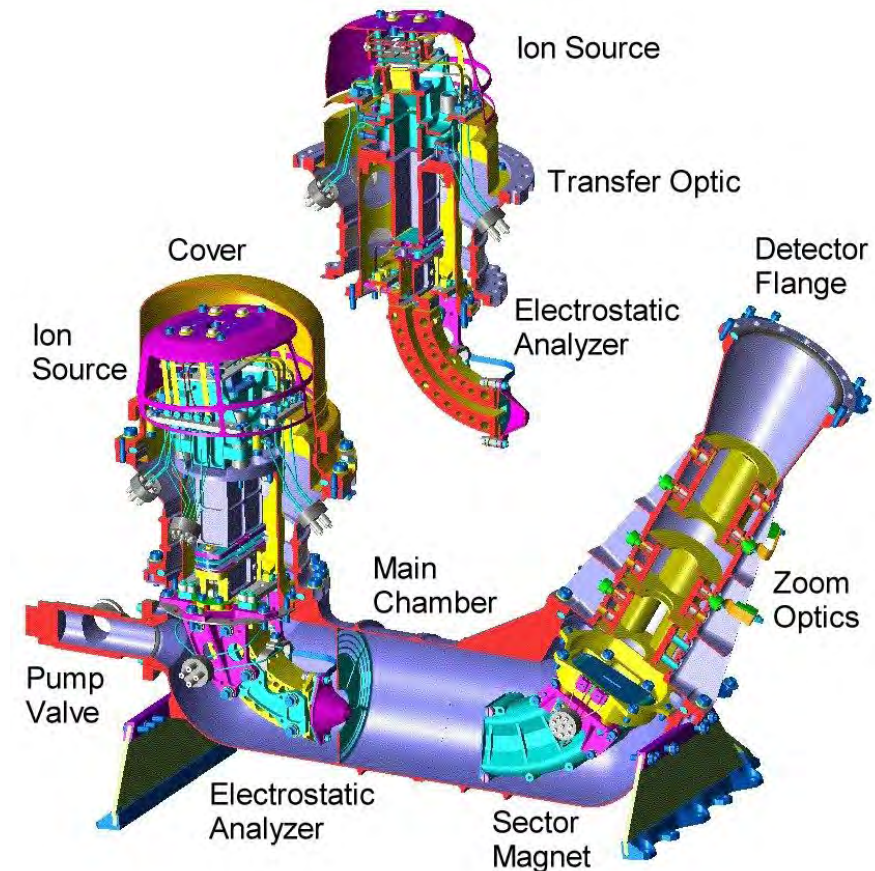
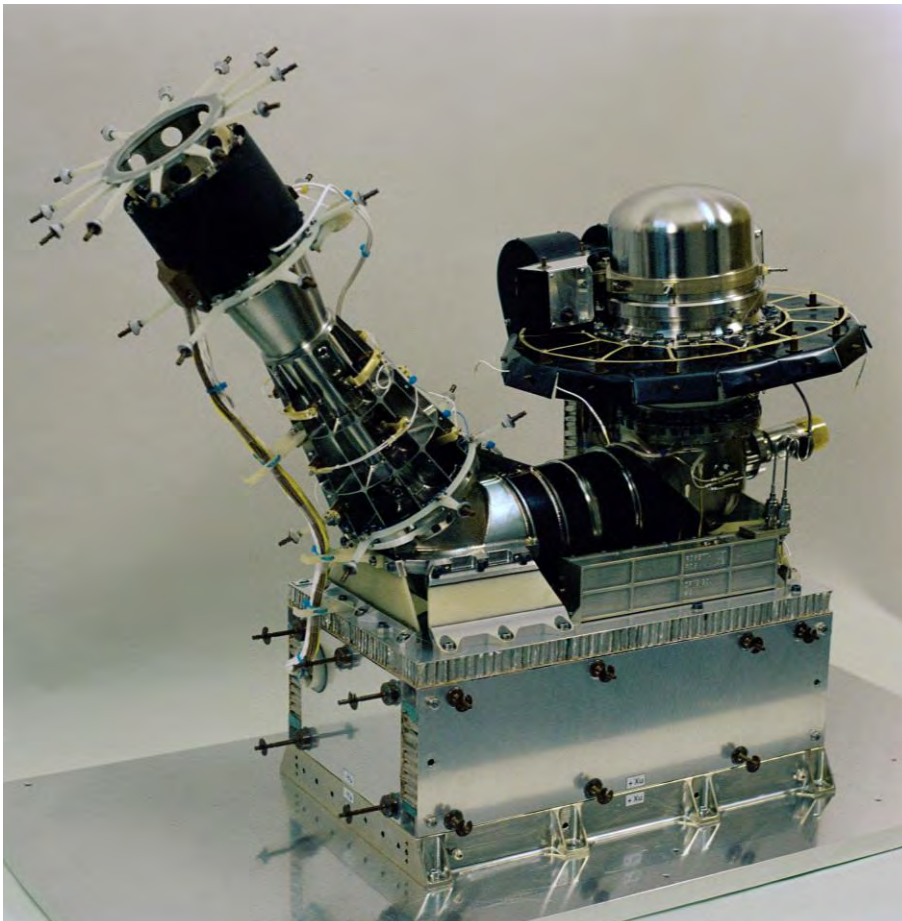
- ❖ $m/\Delta m \approx 100$ (50%)
 - there is separation of low-mass chemical species
- ❖ $m/\Delta m \approx 1000$ (50%)
 - there is a separation of peaks of different nominal mass (e.g., 325 amu versus 326 amu)
- ❖ $m/\Delta m \approx 10'000$ (50%),
 - separation of peaks for nominally isobaric species (i.e., molecules of the same nominal mass differing in elemental composition), e.g., N₂ versus CO, both ~28 amu.
 - resolution of small (< 2500 amu) peptides of the same nominal mass differ by one amino acid (except for isomeric leucine and isoleucine)
- ❖ $m/\Delta m \approx 100'000$ (50%),
 - there is a separation of peaks for nominally isobaric species, e.g. for complex carbon chemistry



P. Wurz, D. Abplanalp, M. Tulej, and H. Lammer,
"A Neutral Gas Mass Spectrometer for the
Investigation of Lunar Volatiles," Planet. Sp.
Science 74 (2012) 264-269.

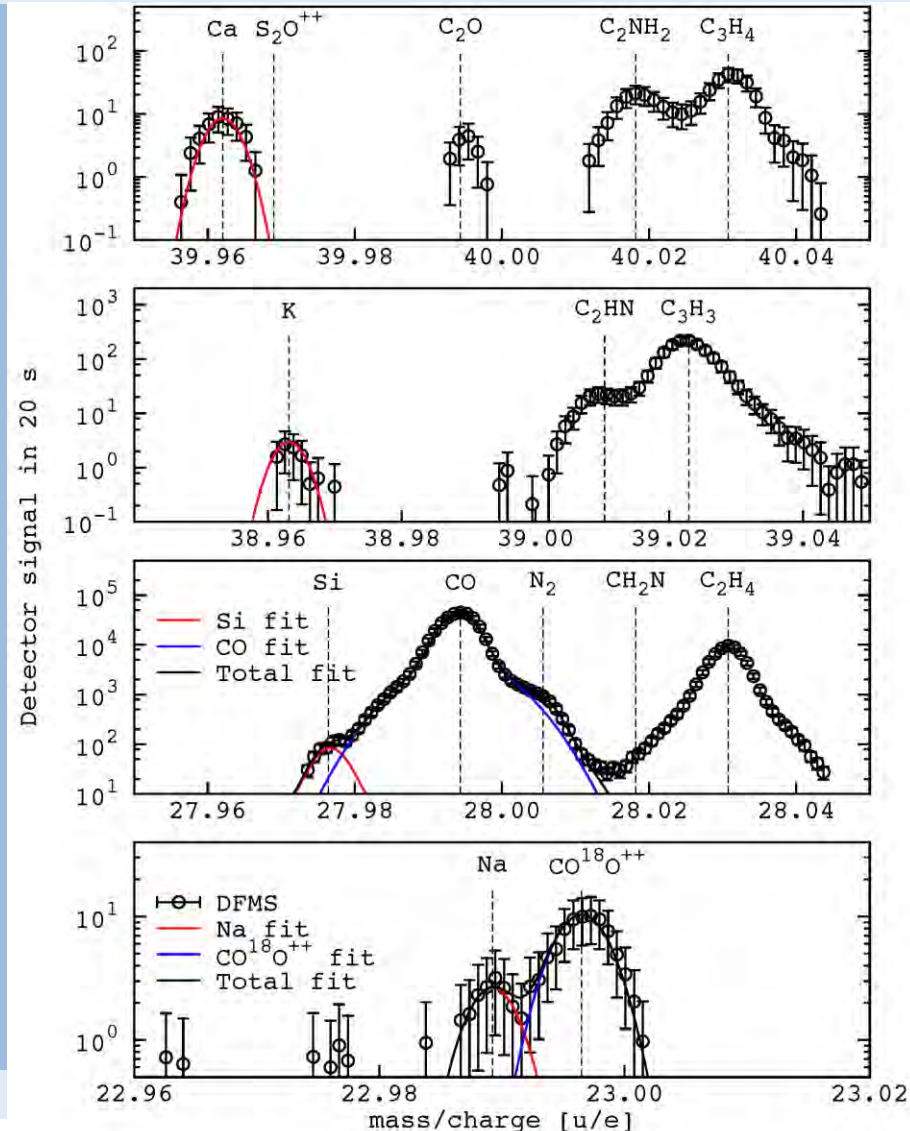
Rosetta / ROSINA / DFMS Instrument

- Covers mass range from 12 to 150 amu/e
- Mass resolution $m/\Delta m > 9000$ (at 50% peak height)
- Detects particle densities of 1 cm^{-3} within 20 s for one mass line
- Complete mass spectrum 20 – 40 min



H. Balsiger, et al., Space Science Review 128 (2007), 745–801.

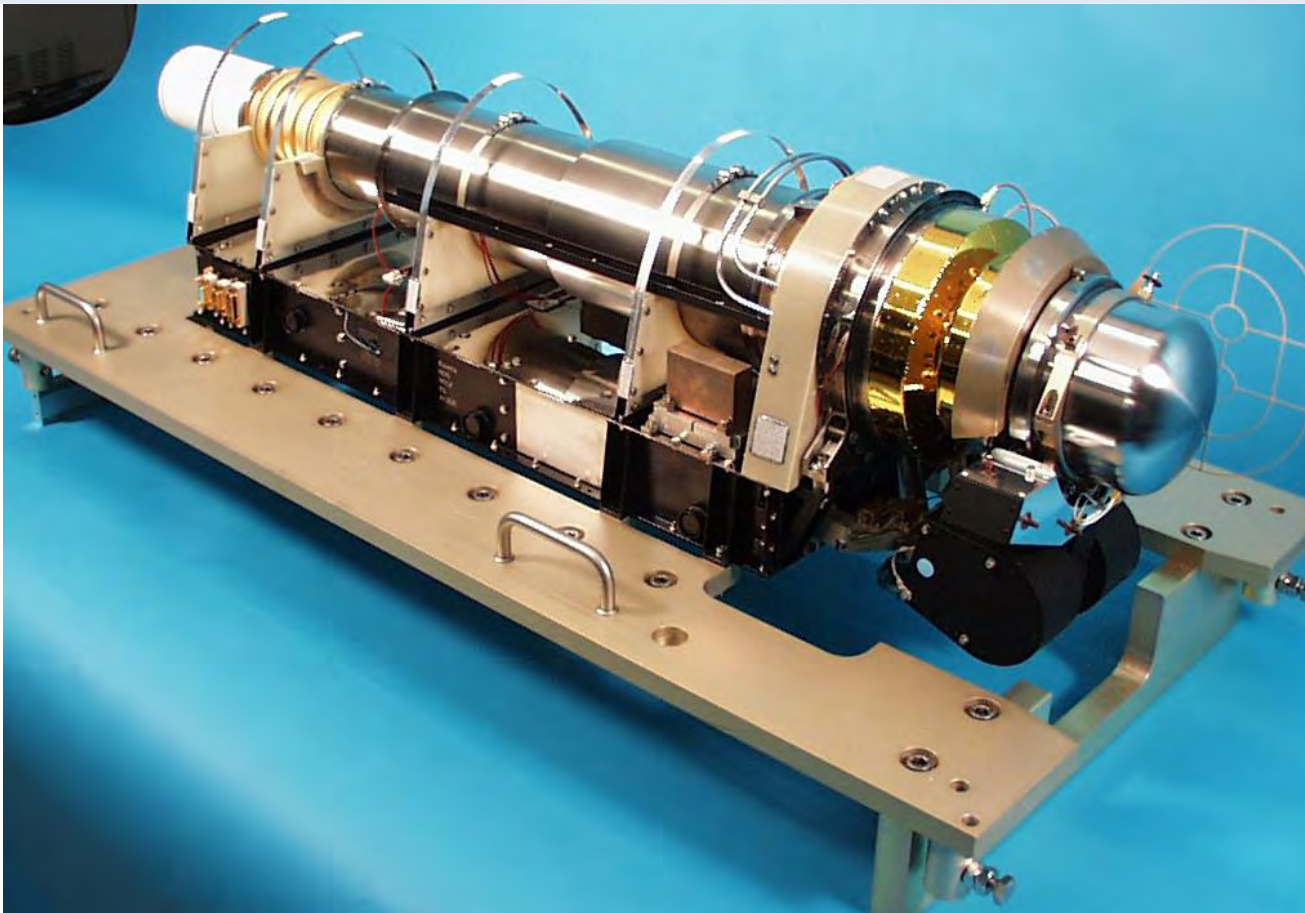
Rosetta / ROSINA Double Focussing Mass Spectrometer (DFMS): Example



The four panels show the high resolution mass spectra from DFMS / ROSINA for the species Ca, K, Si and Na, which are observed together with other species from the volatile material of the coma. Red lines give Gaussian fits to the mass peaks of interest, blue lines to mass peaks that are close to the mass peak of interest, and the black lines are the sum curve.

Wurz et al., A&A 583 (2015) 1–9

RTOF / ROSINA on Rosetta / ESA

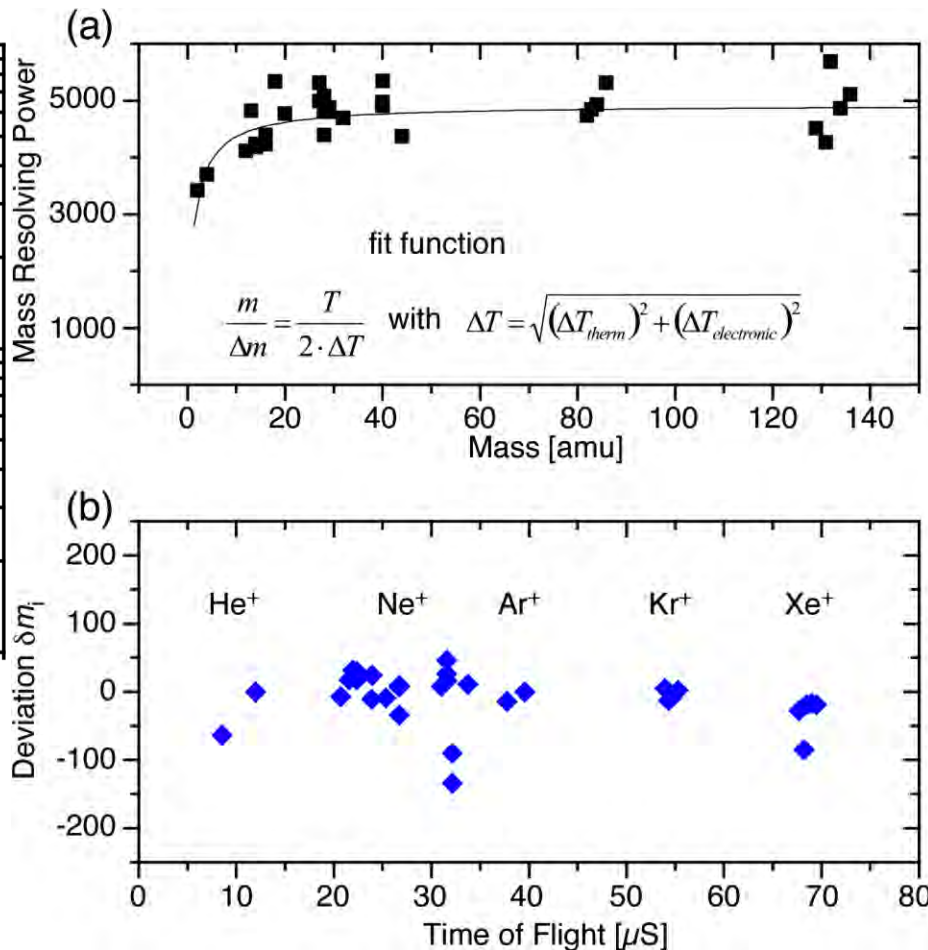
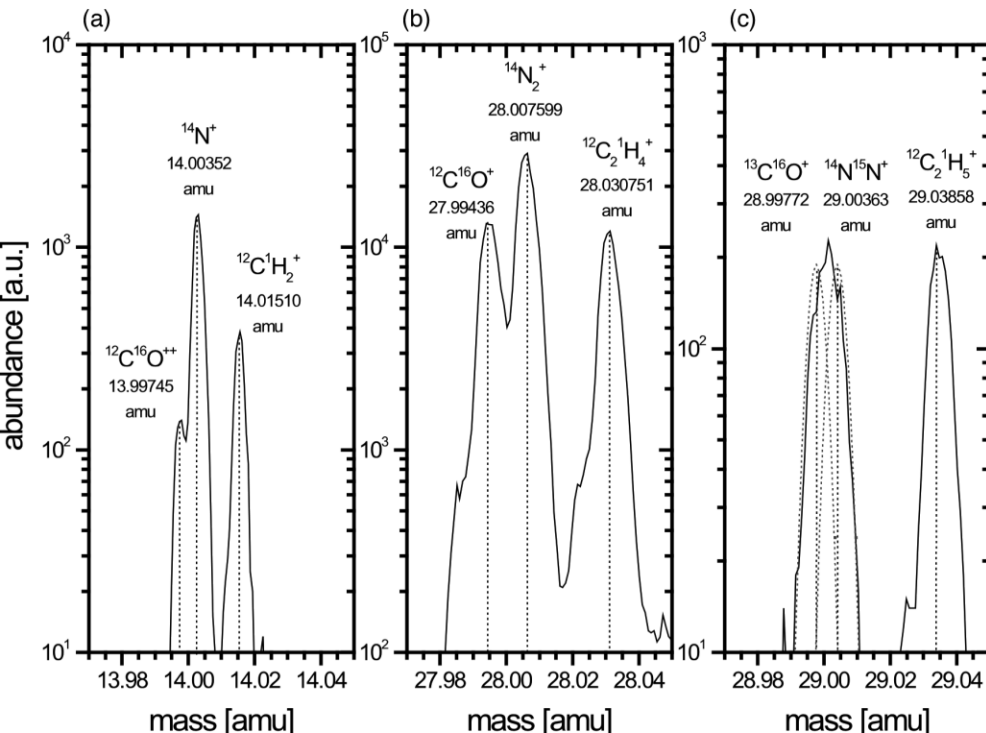


- ❖ RTOF design: 1996
- ❖ Mass resolution:
 $m/\Delta m = 1500 \dots 4500$
(depending on mode)
- ❖ Mass range: 1 ... 500
amu (in principle
unlimited, because
TOF instrument)
- ❖ Sensitivity: $10^{-4} \dots 10^{-3}$
A/mbar (depending on
mode)
- ❖ Mass: 14.7 kg
- ❖ Power: 28 W

H. Balsiger, et al., "ROSINA - Rosetta Orbiter Spectrometer for Ion and Neutral Analysis," Space Science Review 128 (2007), 745–801.

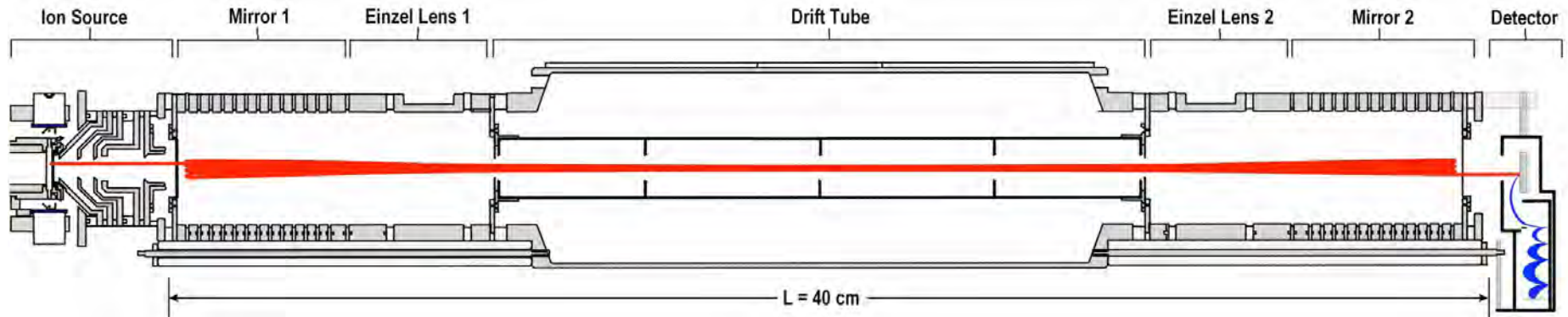
S. Scherer, K. Altwegg, H. Balsiger, J. Fischer, A. Jäckel, A. Korth, M. Mildner, D. Piazza, H. Rème, and P. Wurz, A novel principle for an ion mirror design in time-of-flight mass spectrometry, Int. Jou. Mass Spectr. 251 (2006) 73–81.

Rosetta / ROSINA / RTOF



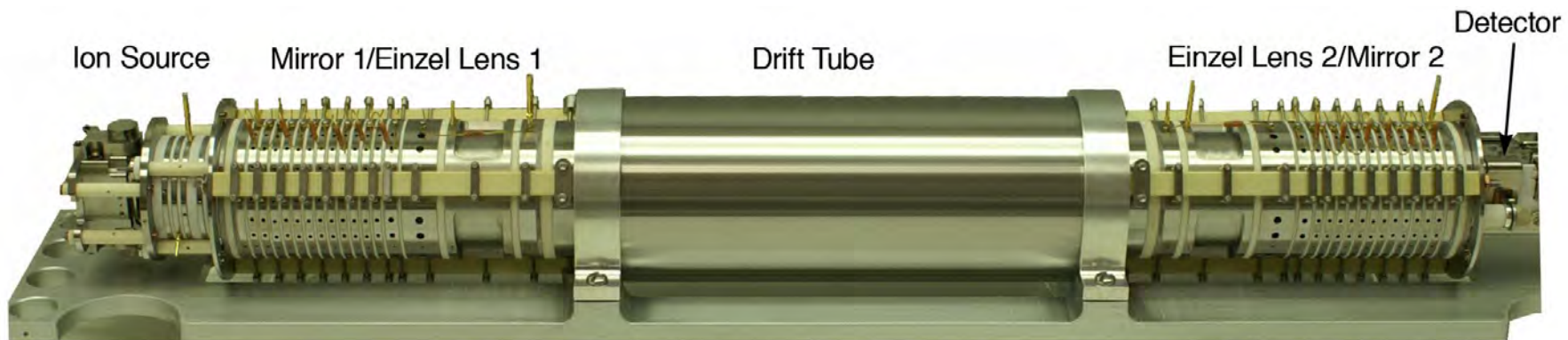
S. Scherer, K. Altwegg, H. Balsiger, J. Fischer, A. Jäckel, A. Korth, M. Mildner, D. Piazza, H. Rème, and P. Wurz,
"A novel principle for an ion mirror design in time-of-flight mass spectrometry," Int. Jou. Mass Spectr. 251 (2006)
73-81.

Multi-Bounce time-of-flight mass spectrometer (MASPEX) Ion Optics Simulations and Prototype



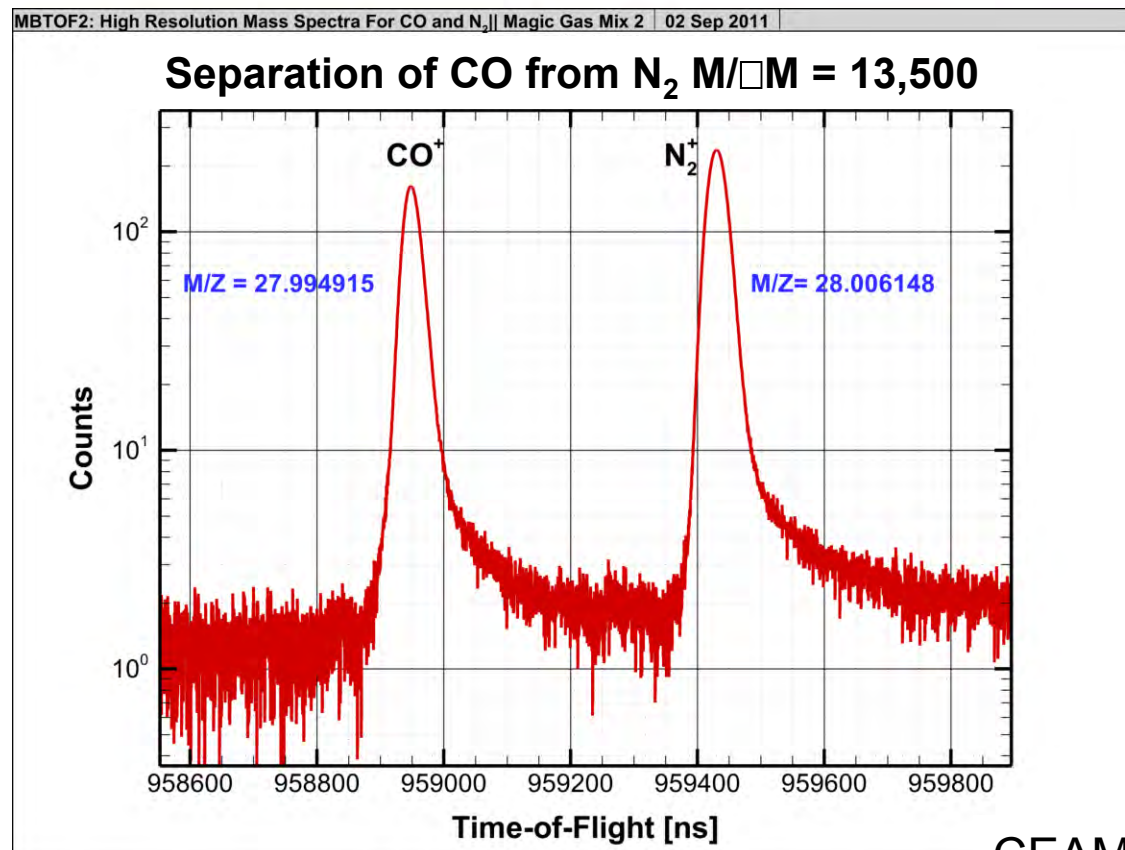
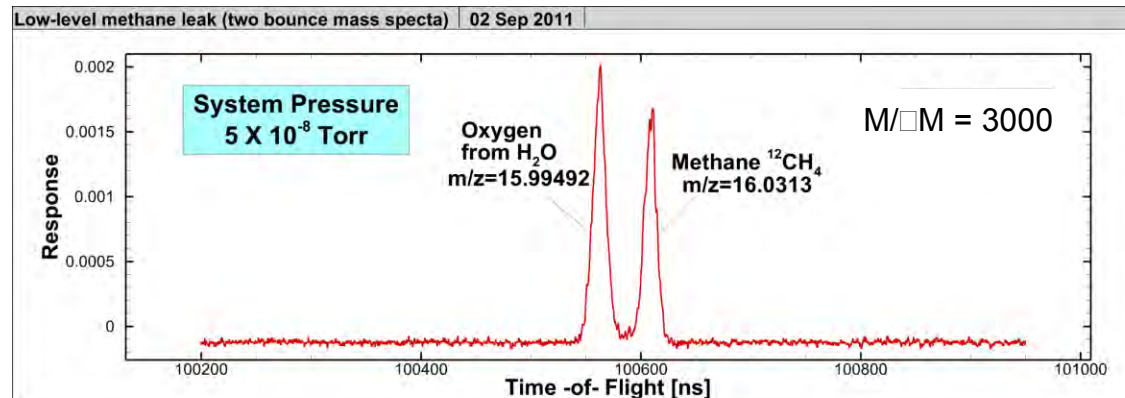
Numerical simulations of ion trajectories showing focusing of multi-bounce ion packets.

$$m/\Delta m(N) = NT_0/2(\Delta t + N\delta T)$$



Third generation MBTOF has successfully undergone vacuum and vibration tests.

MASPEX Performance (High-Resolution Mode)



Orbitrap Mass Sp

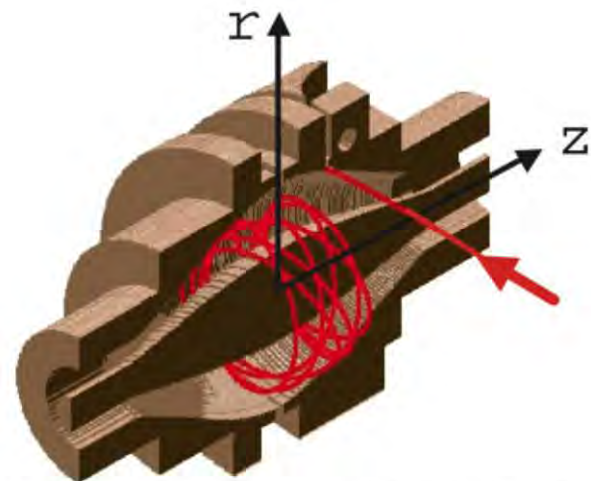


Figure 1. Cutaway view of the Orbitrap mass analyzer. Ions are injected into the Orbitrap at the point indicated by the red arrow. The ions are injected with a velocity perpendicular to the long axis of the Orbitrap (the z-axis). Injection at a point displaced from $z = 0$ gives the ions potential energy in the z-direction. Ion injection at this point on the z-potential is analogous to pulling back a pendulum bob and then releasing it to oscillate.

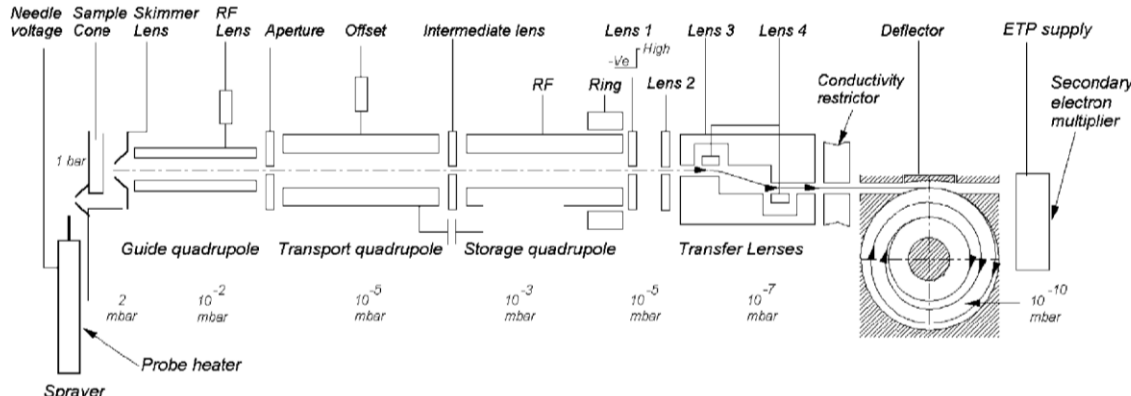
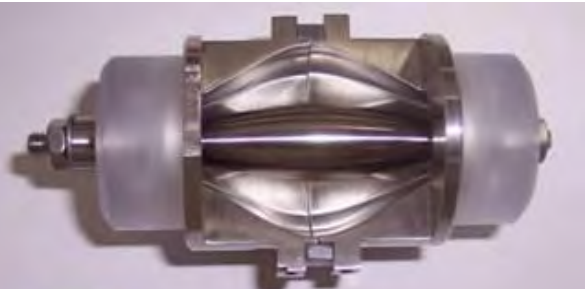


Figure 2. The experimental Orbitrap mass spectrometer. Ions are produced by the electrospray ion source at the extreme left. Ions then proceed through the source, collision quadrupole, selection quadrupole and then pass into the storage quadrupole. The storage quadrupole serves as an ion accumulator and buncher, allowing a pulsed mass analyzer such as the Orbitrap to be coupled to a continuous source like an electrospray ionization source. After accumulation and bunching in the storage quadrupole, the exit lens ('Lens 1') is pulsed low, the ion bunches traverse the ion transfer lens system and are injected into the Orbitrap mass analyzer (shown end-on).

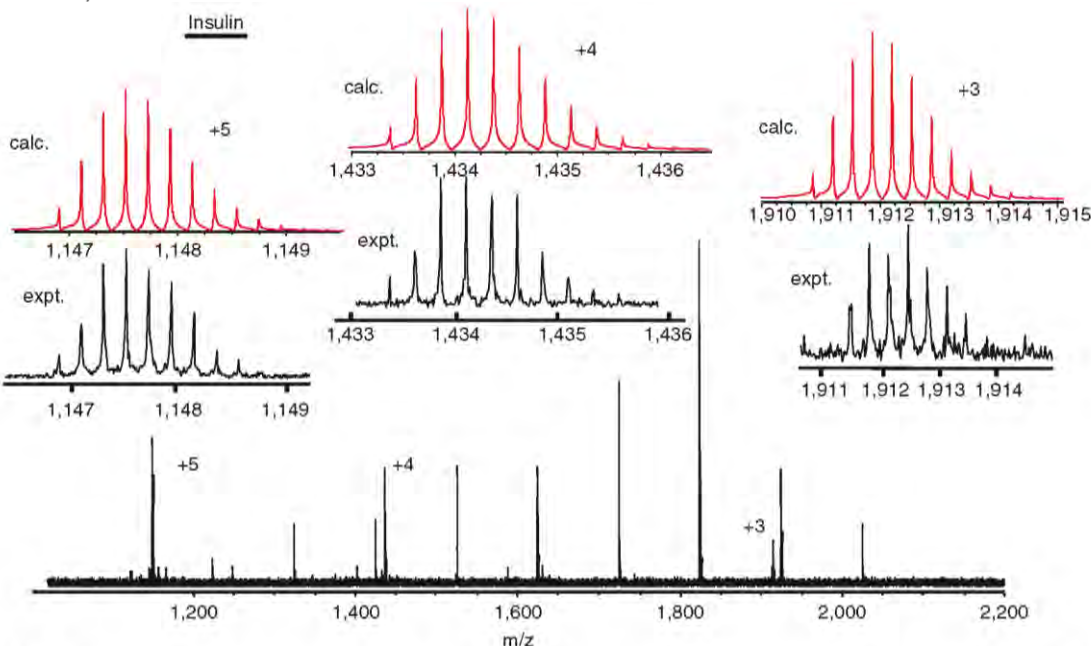
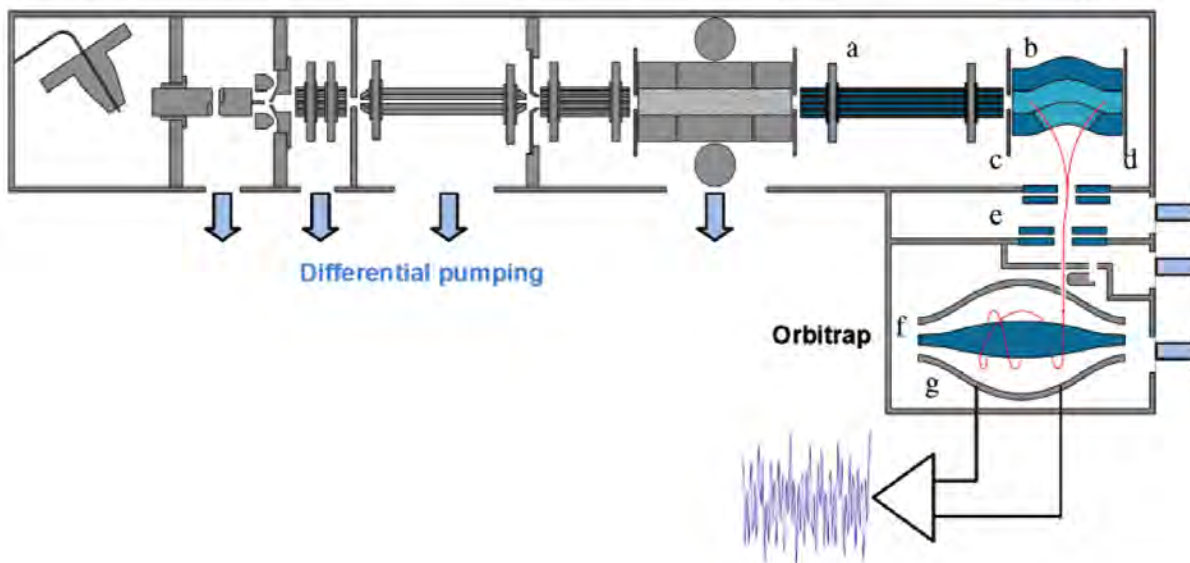
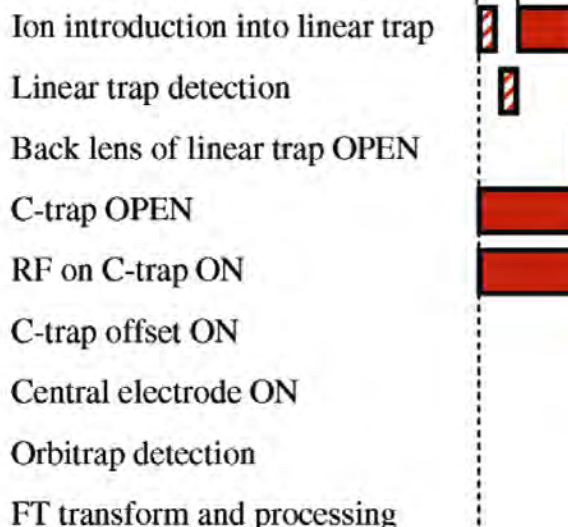


Figure 8. ESI mass spectrum of bovine insulin. Data acquisition parameters include a data sampling rate of 5 MHz, record length was 8 million data points, and the Fourier transform was performed with no apodization function or zero-filling. The lower spectrum shows a wide range mass spectrum including the internal mass calibrant Ultramark 1621 whose oligomers are spaced by 100 mass/charge unit intervals. Lower traces in the close-ups show experimentally obtained isotopic distributions for each charge state. Upper traces in the close-ups show the theoretically expected isotopic distributions. The calculated isotope distributions were obtained from IsoPro 3.0 using Gaussian peak shapes with resolution of 100 000.

(A) API Ion source**(B)**

A. Makarov, E. Denisov, A. Kholomeev, W. Balschun, O. Lange, K. Strupat, and S. Horning, Performance Evaluation of a Hybrid Linear Ion Trap/Orbitrap Mass Spectrometer, *Anal. Chem.*, 78 (2006) 2113-2120.

Figure 1. (A) Schematic layout of the LTQ orbitrap mass spectrometer: (a) Transfer octapole; (b) curved rf-only quadrupole (C-trap); (c) gate electrode; (d) trap electrode; (e) ion optics; (f) inner orbitrap electrode; (g) outer orbitrap electrodes. (B) Simplest operation sequence of the LTQ orbitrap mass spectrometer (not shown are the following: optional additional injection of internal calibrant; additional MS or MS^n scans of linear trap during the orbitrap detection)

Micro-Gas Chromatography Systems (GC-GC)

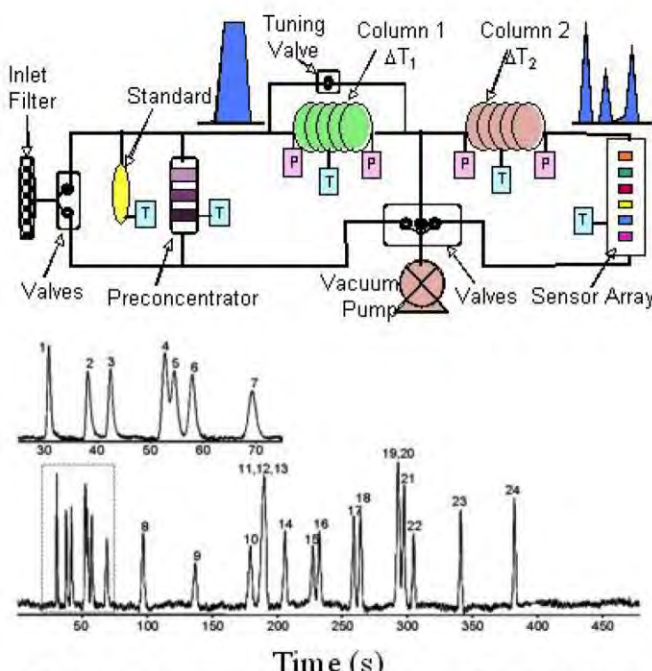


Fig. 1: Block diagram of a microfabricated chromatography-based gas analyzer (above), with a chromatogram on the separation of air-phase petroleum hydrocarbons.

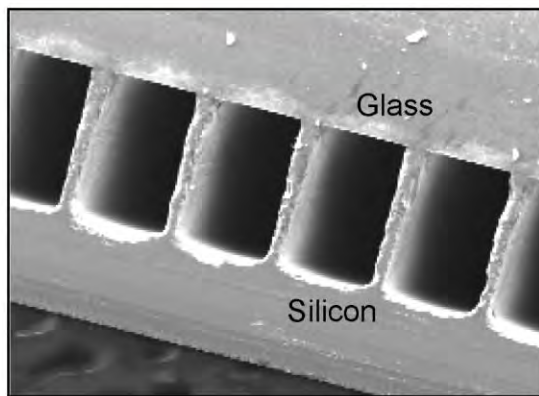
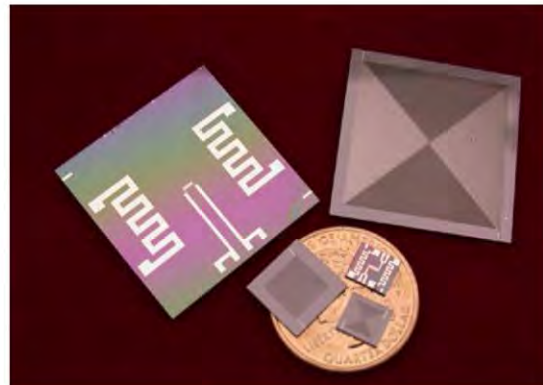


Fig. 4: 2D-GC columns (3m, 25cm, and 10cm) having optimized dimensions on a U.S. quarter, with heaters and sensors to allow closed-loop temperature program on their back surfaces.

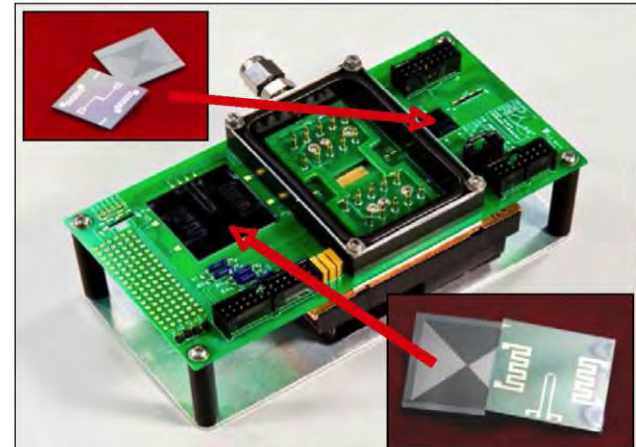


Fig. 6: The GCxGC system, with insets of the first-dimension column (bottom right) and the second-dimension column (top left).

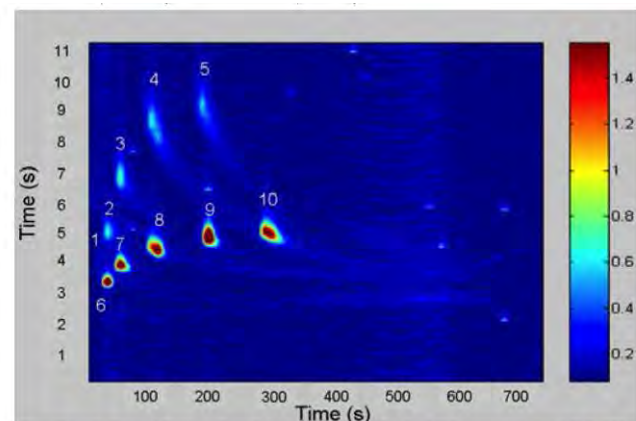
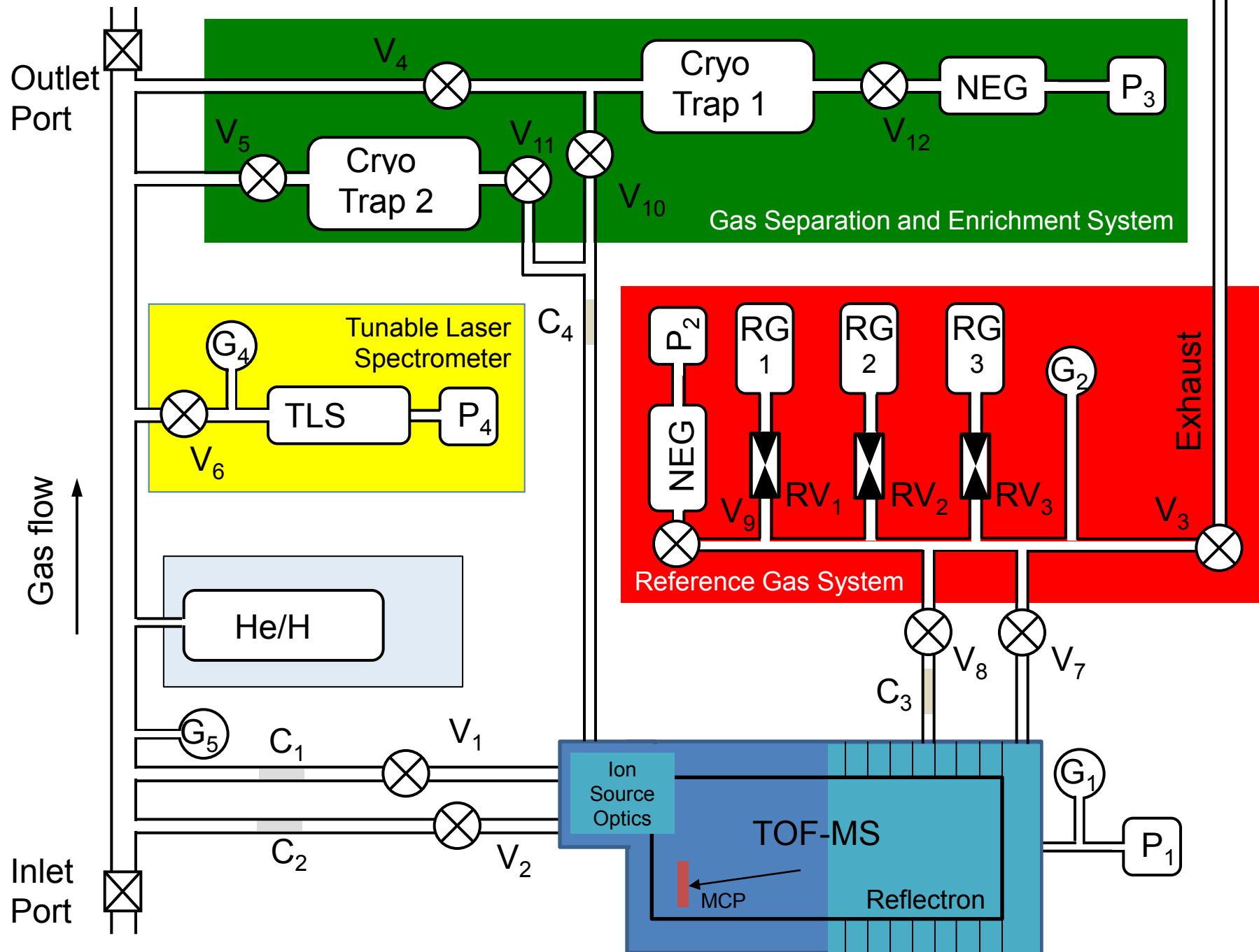


Fig. 7: A two-dimensional contour plot of a 10-component GCxGC separation using 3m- and 0.25m-long microcolumns and a two-stage thermal modulator. Alkanes are separated primarily by the first column (x-axis) and the ketones are separated primarily by the second column (y-axis). Color reflects peak height on the FID.

S. Reidy, S.-J. Kim, K. Beach, B. Block, E.T. Zellers, K. Kurabayashi, and K.D. Wise, A micro-fabricated two-dimensional gas chromatography system, 2010



Possible Implementation for an Atmospheric Probe

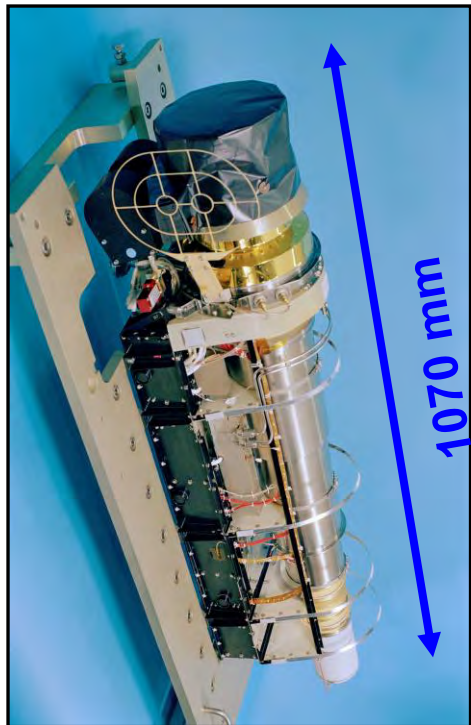
- ❖ Atmospheric composition complex
 - Mass spectrometer
 - Enrichment cells, e.g. Cryo trap
 - Chemical pre-separation
 - TLS, He/H
- ❖ Sufficient sensitivity and vertical resolution
 - Non-scanning instruments → Time of Flight instrument
- ❖ Mass resolution and mass range
 - Not critical
 - Several mass analyser options
- ❖ Limit complexity
 - Simple Time of Flight instrument
 - Traps
 - Chemical pre-separation
- ❖ Limit instrument resources

u^b

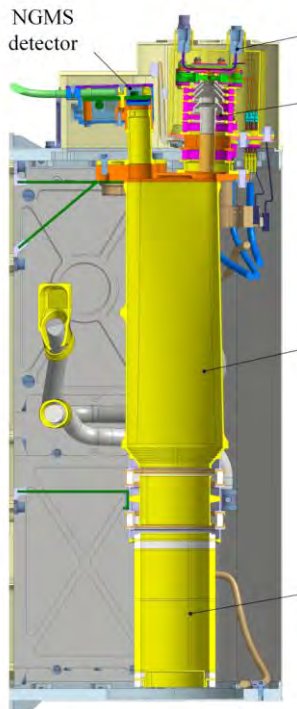
b
UNIVERSITÄT
BERN

Technological Development

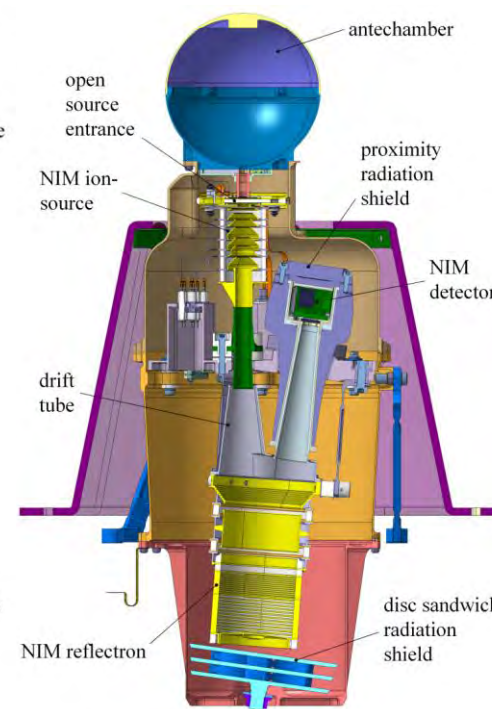
RTOF / ROSINA /
Rosetta
1997



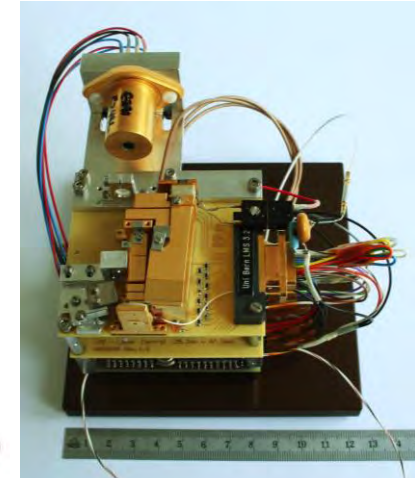
NGMS / GC-MS /
Luna-Resurs
2010



NIM / PEP / JUICE
2016



LMS / Rover
BepiColombo
2003



RTOF Mass: 15 kg
Mean Power 30 W

NGMS Mass: 3.5 kg
Mean Power 25 W

NIM Mass: 2.5 kg
Shielding: 2.8 kg
Mean Power 10.3 W

LMS Mass: 0.5 kg
Mean Power 3.0W

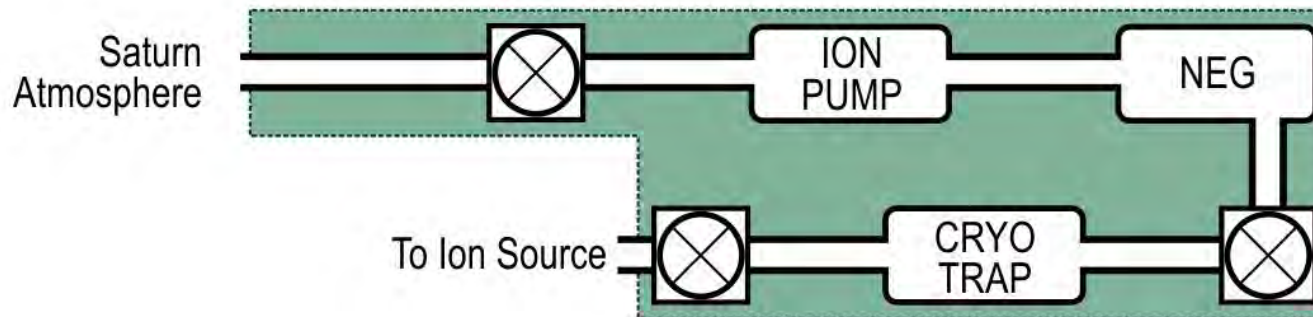
Possible Future Developments

- ❖ Increase in sensitivity
- ❖ Increased mass range
- ❖ Increase in mass resolution
- ❖ Reduced complexity
- ❖ Reduced instrument resources

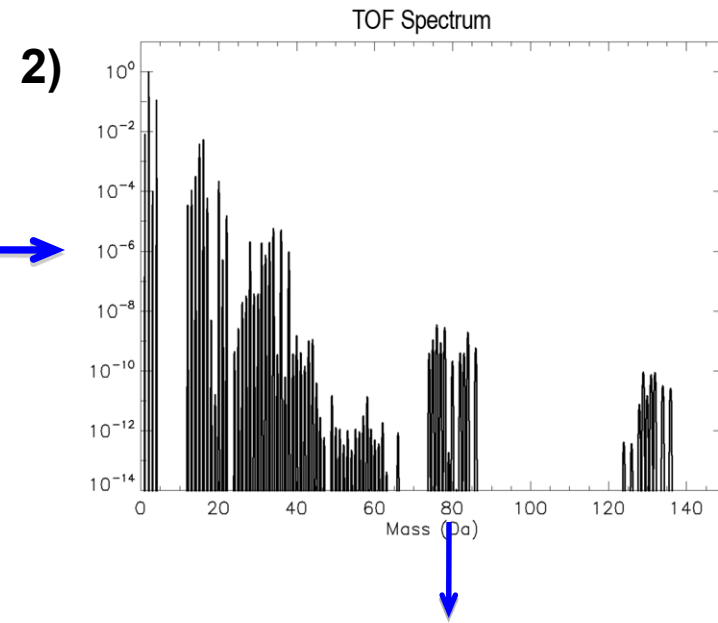
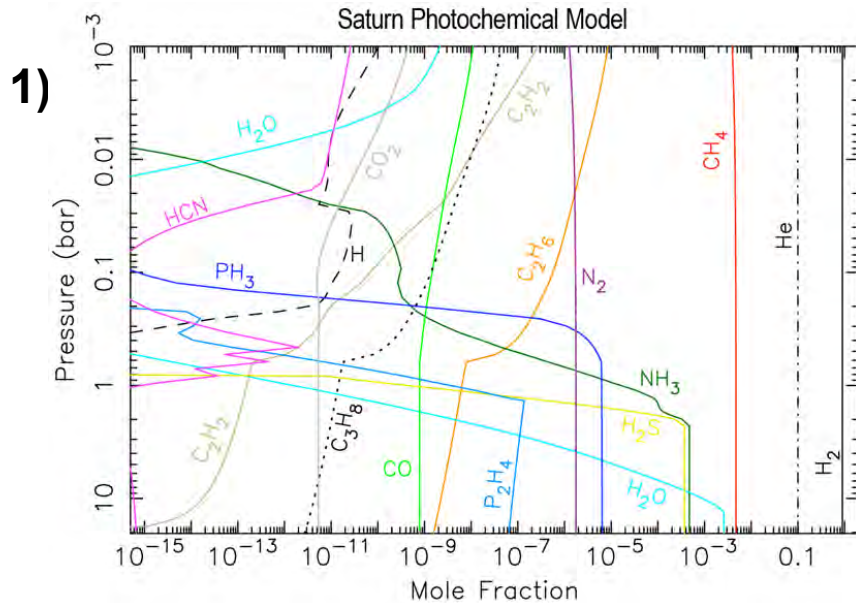
Noble Gas Sample Concentration: Cryotrap

❖ Sample concentration

- Even though a TOF-MS is over 1000 times more sensitive than Cassini INMS (10x from ion source efficiency and 100 x from better duty cycle), calculations show that it would take longer than the probe descent time to provide the counting statistics required for the isotopes of Kr and Xe with sufficient accuracy
- The noble gas enhancement can be achieved by using a combination of a cryotrap, ion pump, and non-evaporable getter (NEG: SAES 172).
- The NEG removes all constituents except methane and the noble gases.
- The cryotrap traps the products of the NEG process, except for helium and some neon.
- The ion pump then operates to pump away the helium, which is the second highest source of gas, thus enhancing the remaining noble gases ~ 200 times.
- Helium and neon are measured using a separate mode.



Scientific Requirements



STEP 1: Saturn atmosphere model (J. Moses) produced as the basis for estimating the mass spectrometric measurement requirements (over 100 compounds from 0.5 to 20 bars).

STEP 2: Simulated mass spectrum generated using empirical laboratory data (line shapes) from mass spectrometer combined with NIST fragmentation and ionisation data and solar isotopic abundance information (H. Waite).

STEP 3: Spreadsheet programme developed to determine mass resolution and measurement time needed to satisfy the requirements and thus generate a realistic operational scenario (H. Waite).

3)

Results for the Measurement of Ambient Gas at 0.5 bar

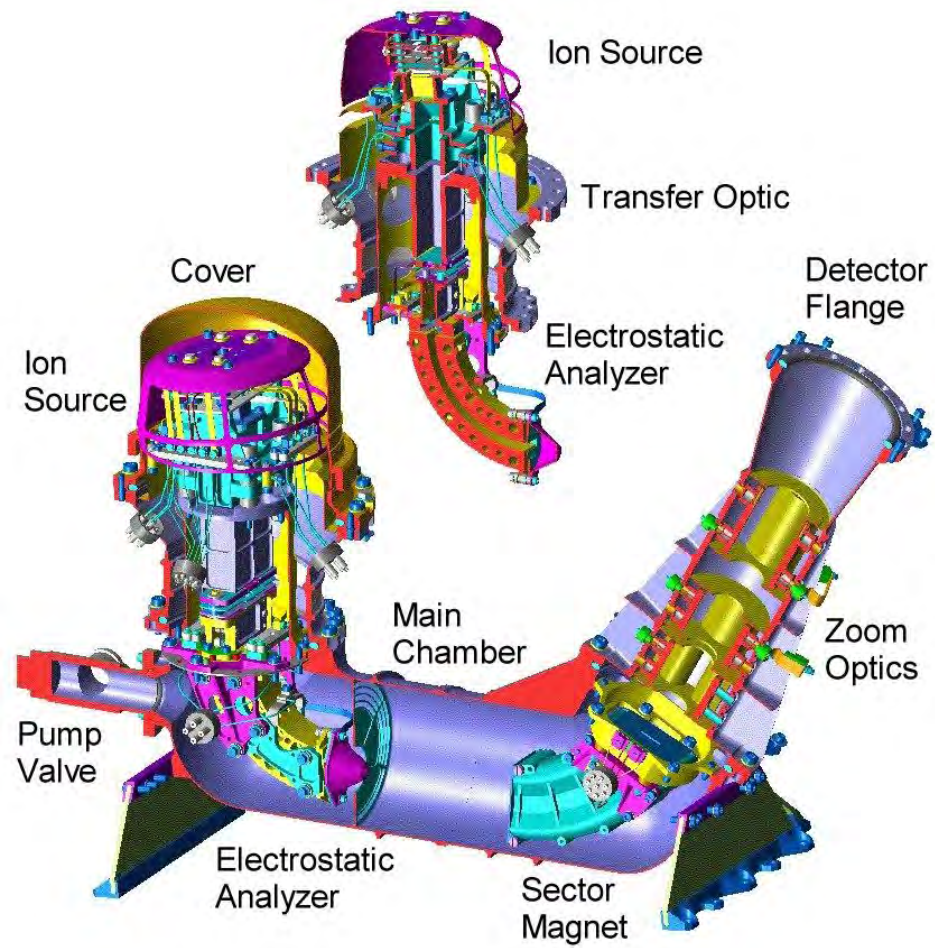
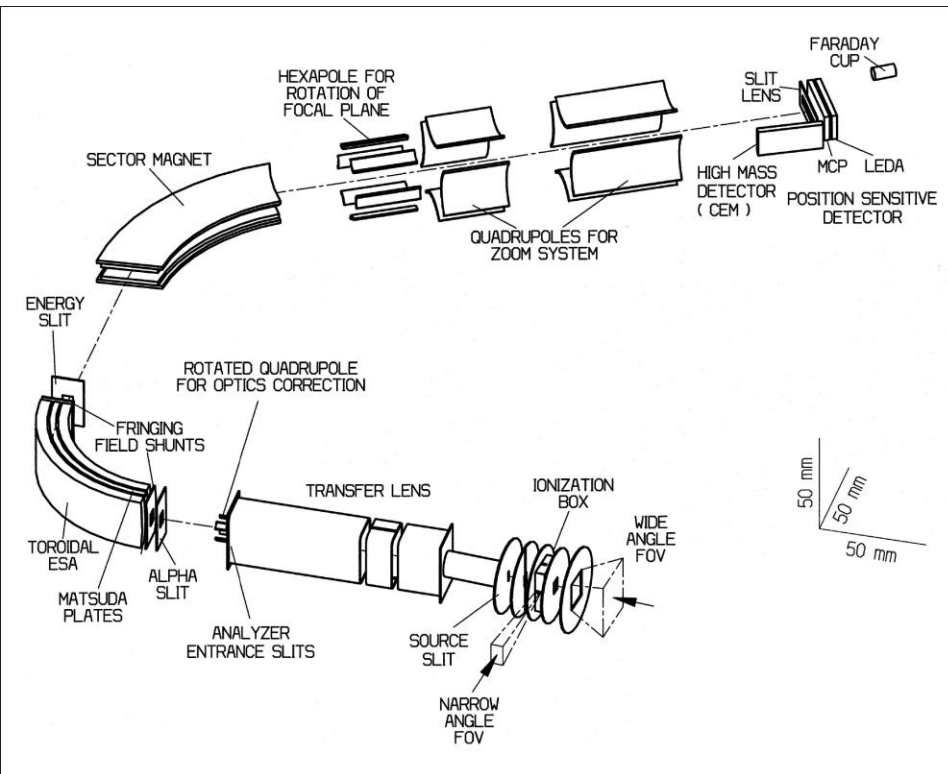
Molecule	Specific isotope	Exact mass g/mol	Principal isotope	Molecular abundance	Mixing fraction	Min required acquisition time sec	Target precision	Minimum bounces required
<i>RMN</i>								
H ₂	¹ H ₂	2.0	P	0.895	0.895	<0.1	5%	0
H ₂	¹ H/ ³ H	3.0	² H	0.895	3.58E-5	<0.1	5%	4
He	³ He	3.0	³ He	0.1	4.04E-5	<0.1	10%	4
He	⁴ He	4.0	P	0.1	0.1	<0.1	5%	0
CH ₄	¹² C/H ₄	16.0	P	0.005	0.005	<0.1	1%	0
CH ₄	¹³ C/H ₄	17.0	¹³ C	0.005	5.25E-5	1.7	1%	0
CH ₄	¹⁴ C/H ₄	17.0	P	0.005	3.72E-7	9.7	5%	21
N ₂	¹⁴ N ₂	28.0	P	1.78E-6	1.74E-6	0.3	10%	3
Ne	²⁰ Ne	20.0	P	2.08E-4	1.92E-4	<0.1	10%	0
Ne	²² Ne	22.0	²² Ne	2.06E-4	1.39E-5	0.2	10%	0
NH ₃	¹⁵ NH ₃	17.0	P	1.39E-7	1.30E-7	7.7	10%	8
Ar	³⁶ Ar	36.0	P	5.37E-6	1.81E-8	21.1	10%	0
Ar	³⁸ Ar	38.0	³⁸ Ar	5.37E-6	3.41E-9	111.7	10%	0
C ₂ H ₆	¹² C/ ¹ H ₆	30.0	P	3.34E-8	3.27E-8	22.19.6	1%	3
C ₂ H ₆	¹³ C/ ¹ H ₆	31.1	¹³ C	3.34E-8	7.38E-10	393205	1%	16
Kr	⁷⁹ Kr	79.9	⁸⁰ Kr	3.04E-9	6.89E-11	13948.3	10%	3
Kr	⁸¹ Kr	81.9	⁸² Kr	3.04E-9	3.51E-10	2734.6	10%	0
Kr	⁸² Kr	82.9	⁸³ Kr	3.04E-9	3.40E-10	2748.1	10%	0
Kr	⁸³ Kr	83.9	P	3.04E-9	1.74E-10	952.4	10%	0
Kr	⁸⁵ Kr	85.9	⁸⁶ Kr	3.04E-9	5.25E-10	1829	10%	0
Xe	¹²⁷ Xe	127.9	¹²⁸ Xe	3.04E-10	2.18E-12	22918.6	10%	0
Xe	¹²⁸ Xe	128.9	P	3.04E-10	2.21E-10	3249.6	10%	0
Xe	¹²⁹ Xe	129.9	¹³⁰ Xe	3.04E-10	4.61E-12	109669.6	10%	0
Xe	¹³⁰ Xe	130.9	¹³¹ Xe	3.04E-10	2.41E-11	20707.4	10%	0
Xe	¹³¹ Xe	131.9	¹³² Xe	3.04E-10	3.05E-11	16409.1	10%	0
Xe	¹³³ Xe	133.9	¹³⁴ Xe	3.04E-10	1.19E-11	42291.8	10%	0
Xe	¹³⁵ Xe	135.9	¹³⁶ Xe	3.04E-10	1.E-11	49875.7	10%	0

u^b

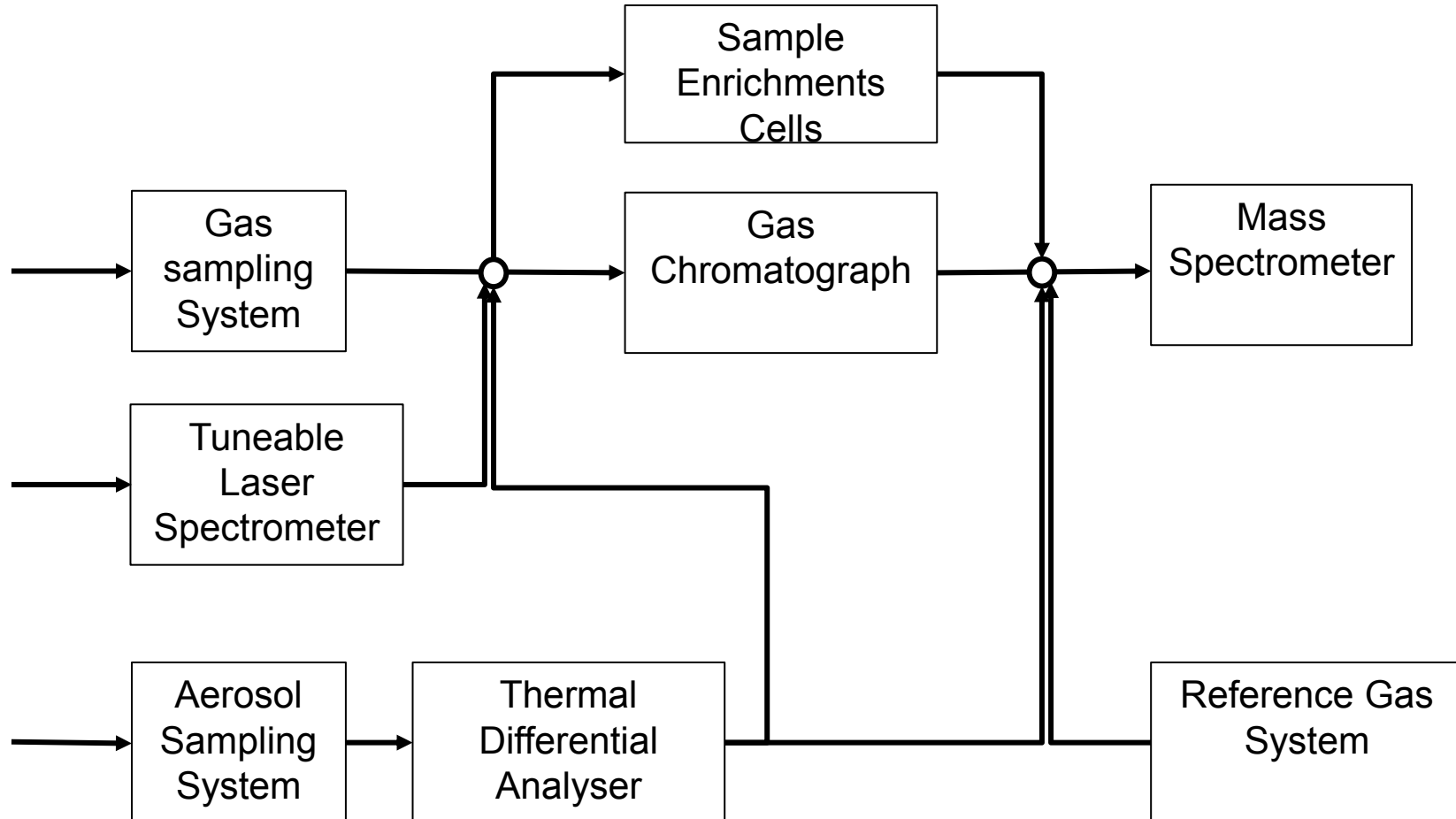
b
UNIVERSITÄT
BERN

Reduced Complexity

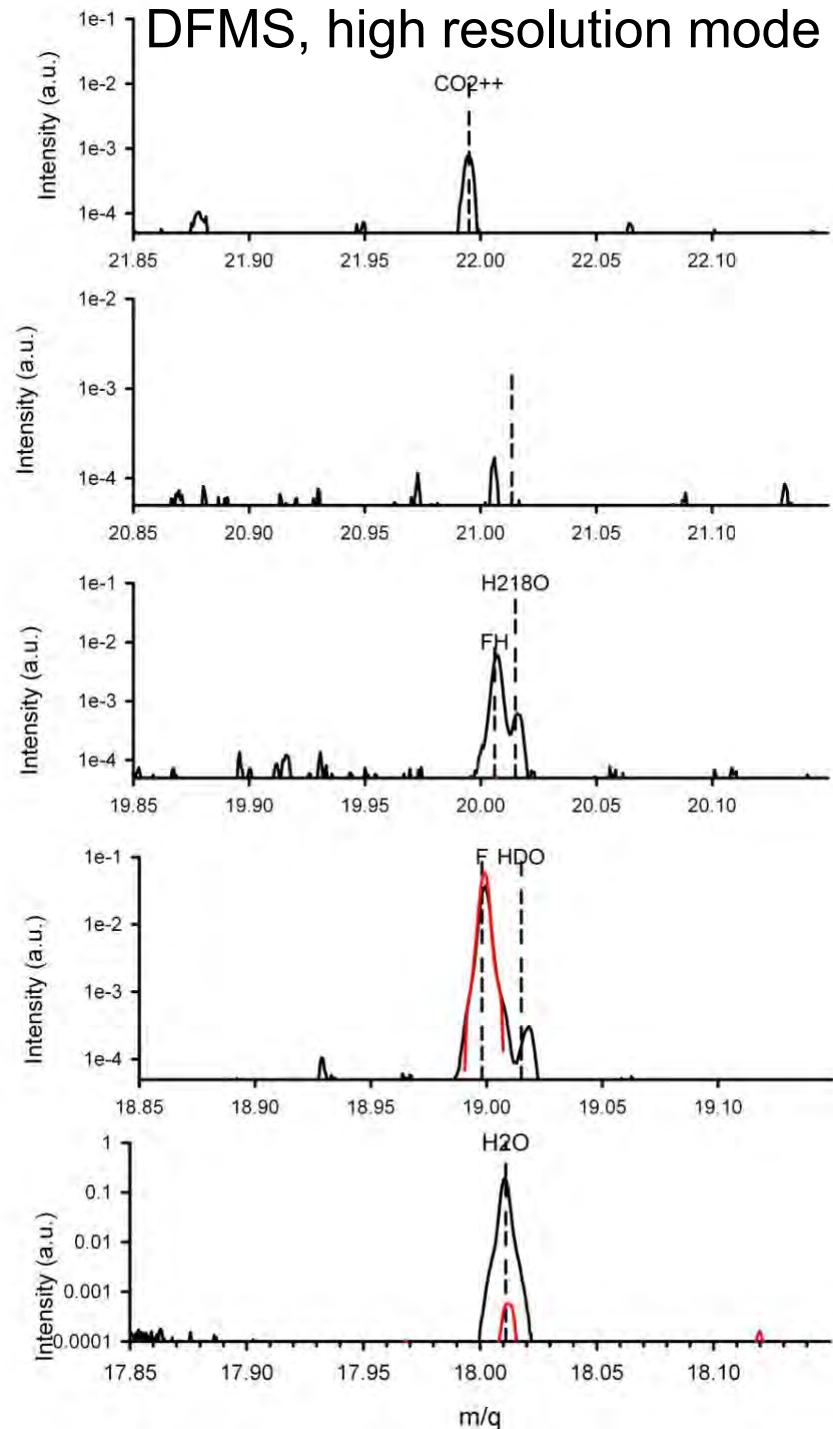
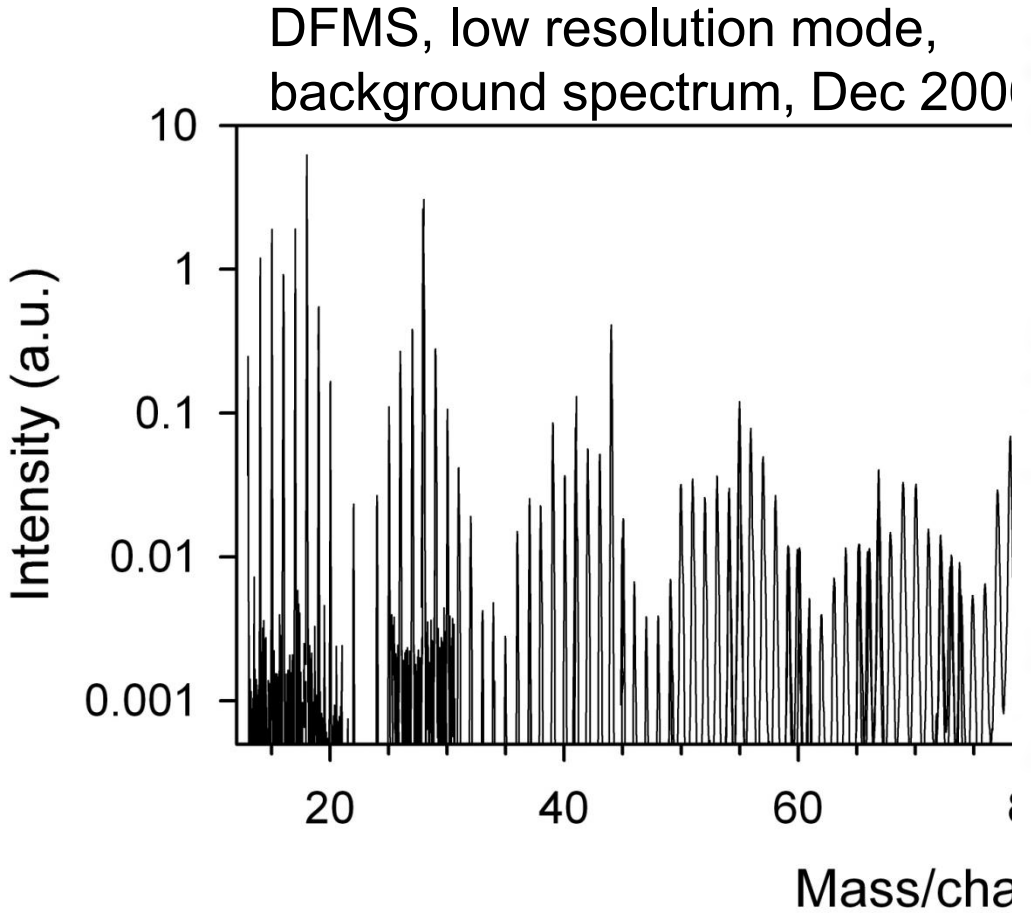
Rosetta / ROSINA / DFMS Sensor



Instrument Overview



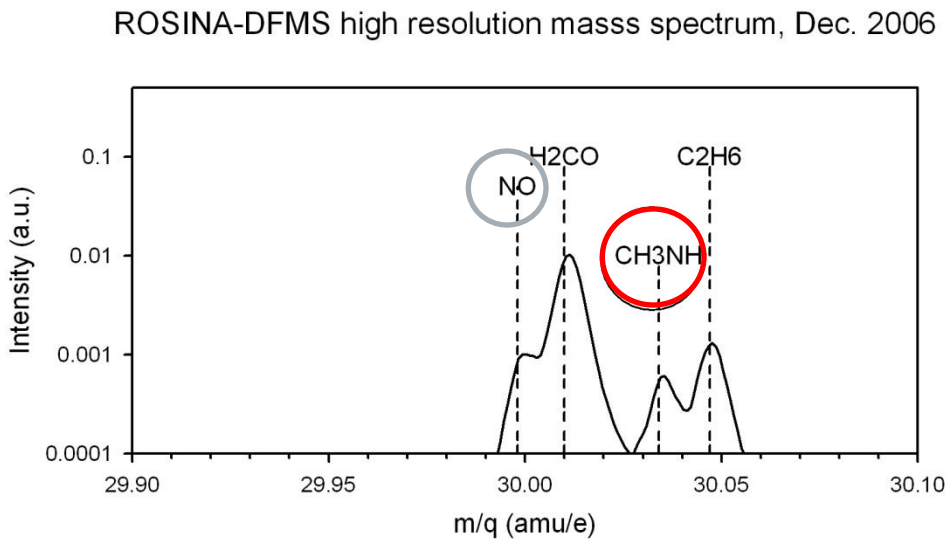
Rosetta / ROSINA: Active comet Double Focussing Mass Spectrometer



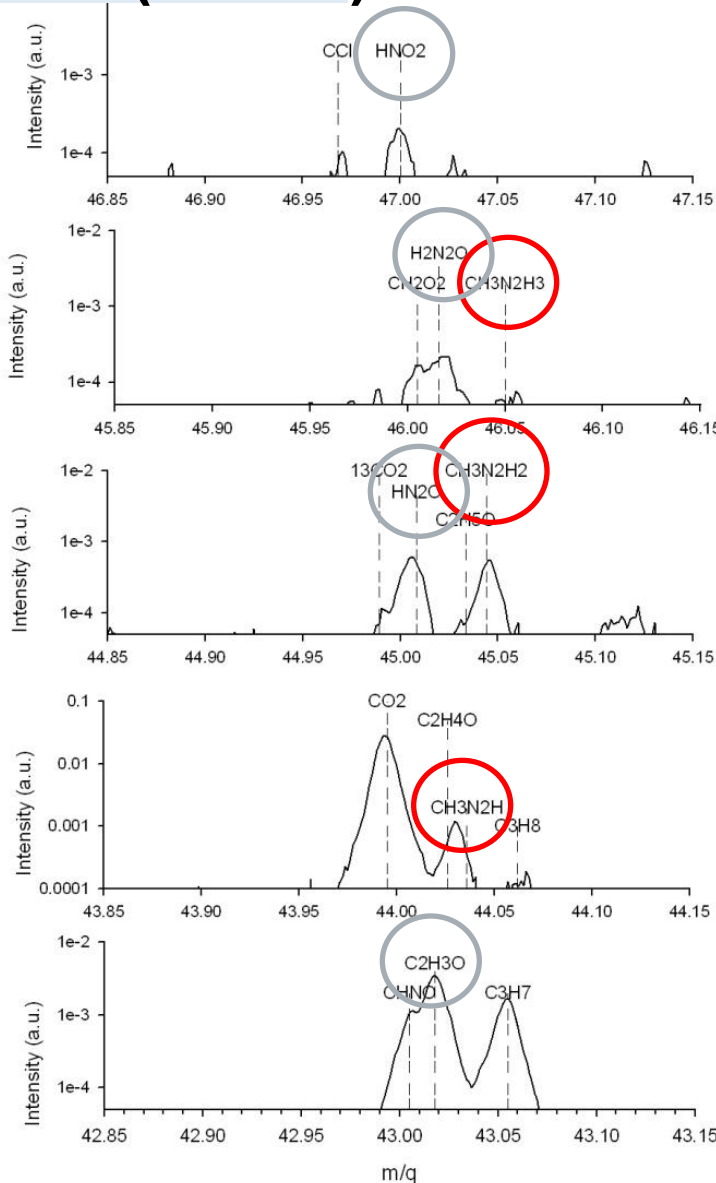
B. Schl  ppi, K. Altwegg, H. Balsiger, M. H  ssig, A. J  ckel, P. Berthelier, J. DeKeyser, H. R  me, and U. Mall, "The influence of tenuous atmospheres with in situ mass spectrometry," Jou. C.

Rosetta / ROSINA: Active checkout PC4 Double Focussing Mass Spectrometer (DFMS)

Traces of hydrazine $\text{CH}_3\text{N}_2\text{H}_3$, its oxidant N_2O_4 , and products, 20 h after thruster firing

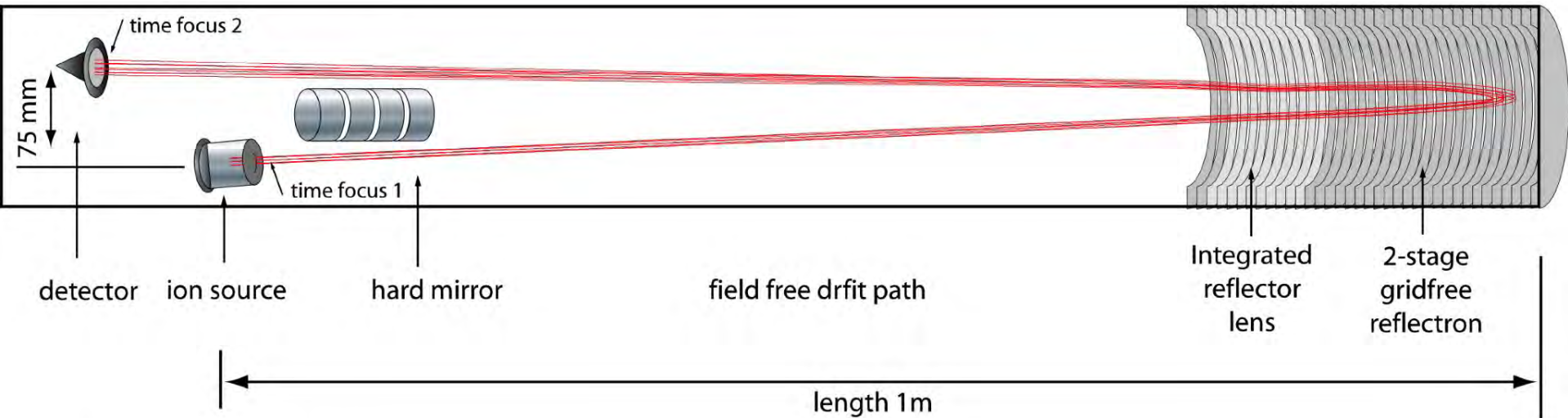


$$P_{\text{total}} \sim 4 \times 10^{-11} \text{ mbar}, P_{\text{hydrazine}} \sim 1 \times 10^{-12} \text{ mbar}$$

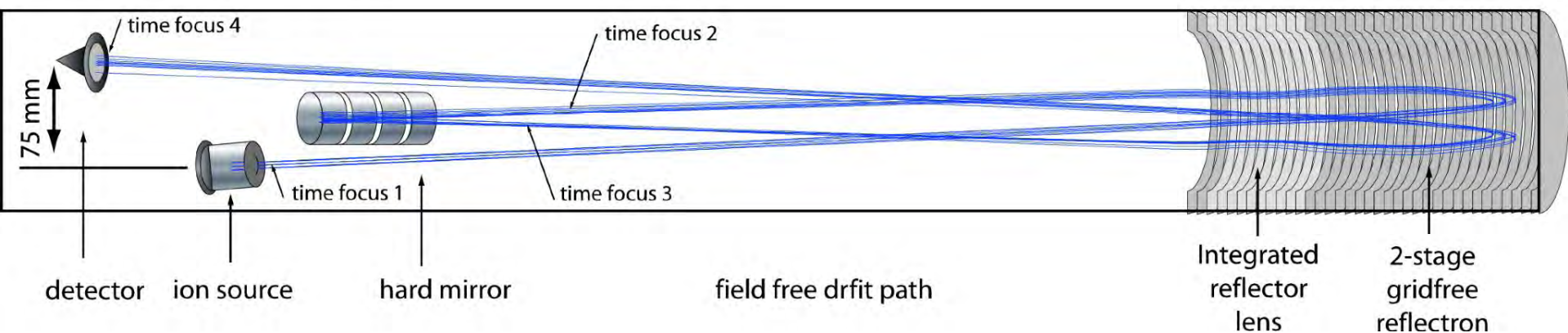


RTOF / ROSINA / Rosetta

a) single reflection mode



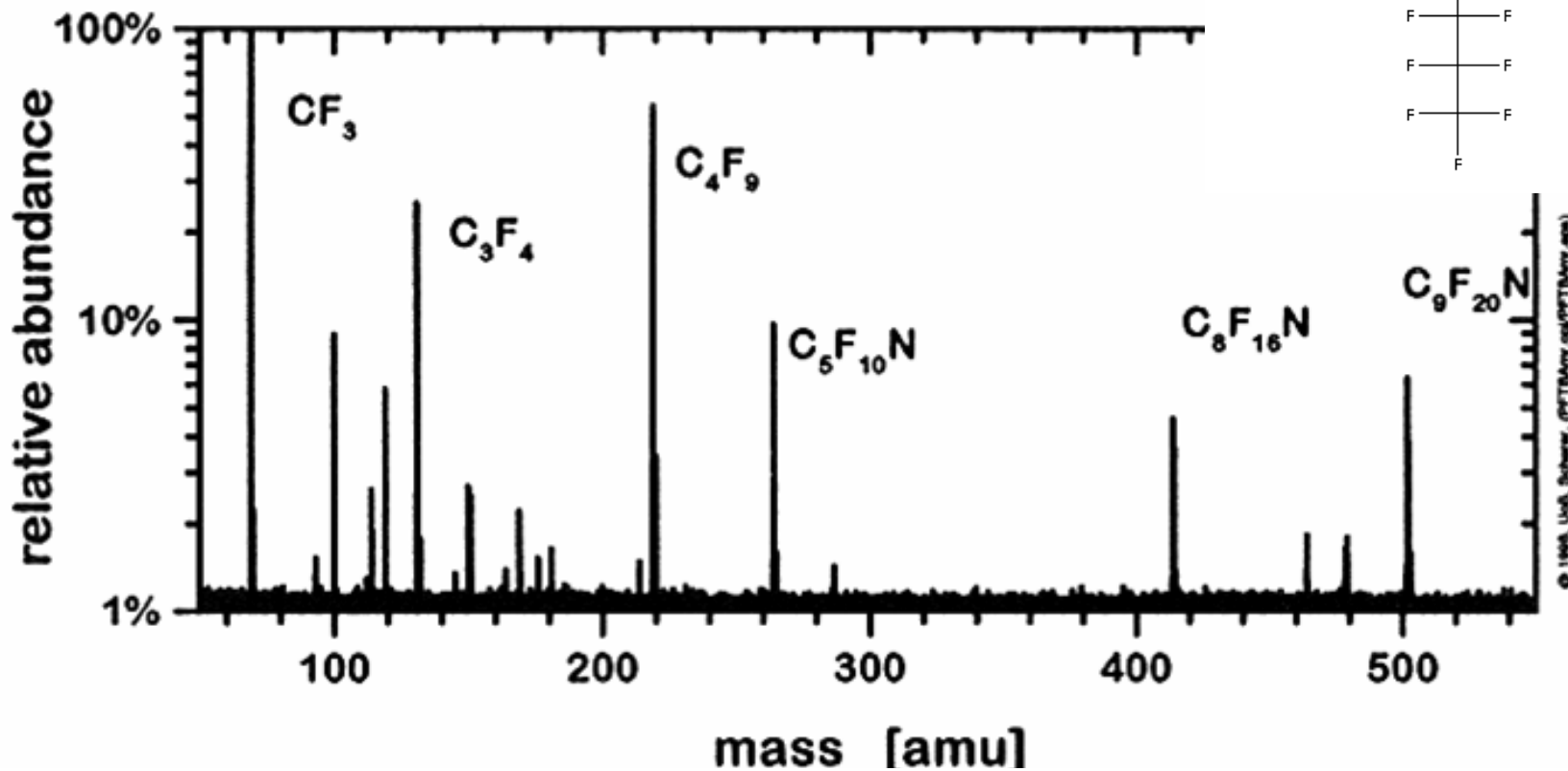
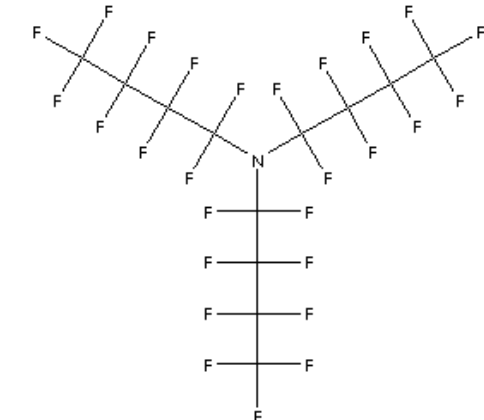
b) triple reflection mode



M. Hohl, P. Wurz, S. Scherer, K. Altwegg, and H. Balsiger, Int. J. Mass Spectr. 188 (1999), 189–197.

S. Scherer, K. Altwegg, H. Balsiger, J. Fischer, A. Jäckel, A. Korth, M. Mildner, D. Piazza, H. Rème, and P. Wurz, Int. Jou. Mass Spectr. 251 (2006) 73–81.

RTOF / ROSINA / Rosetta Mass Range

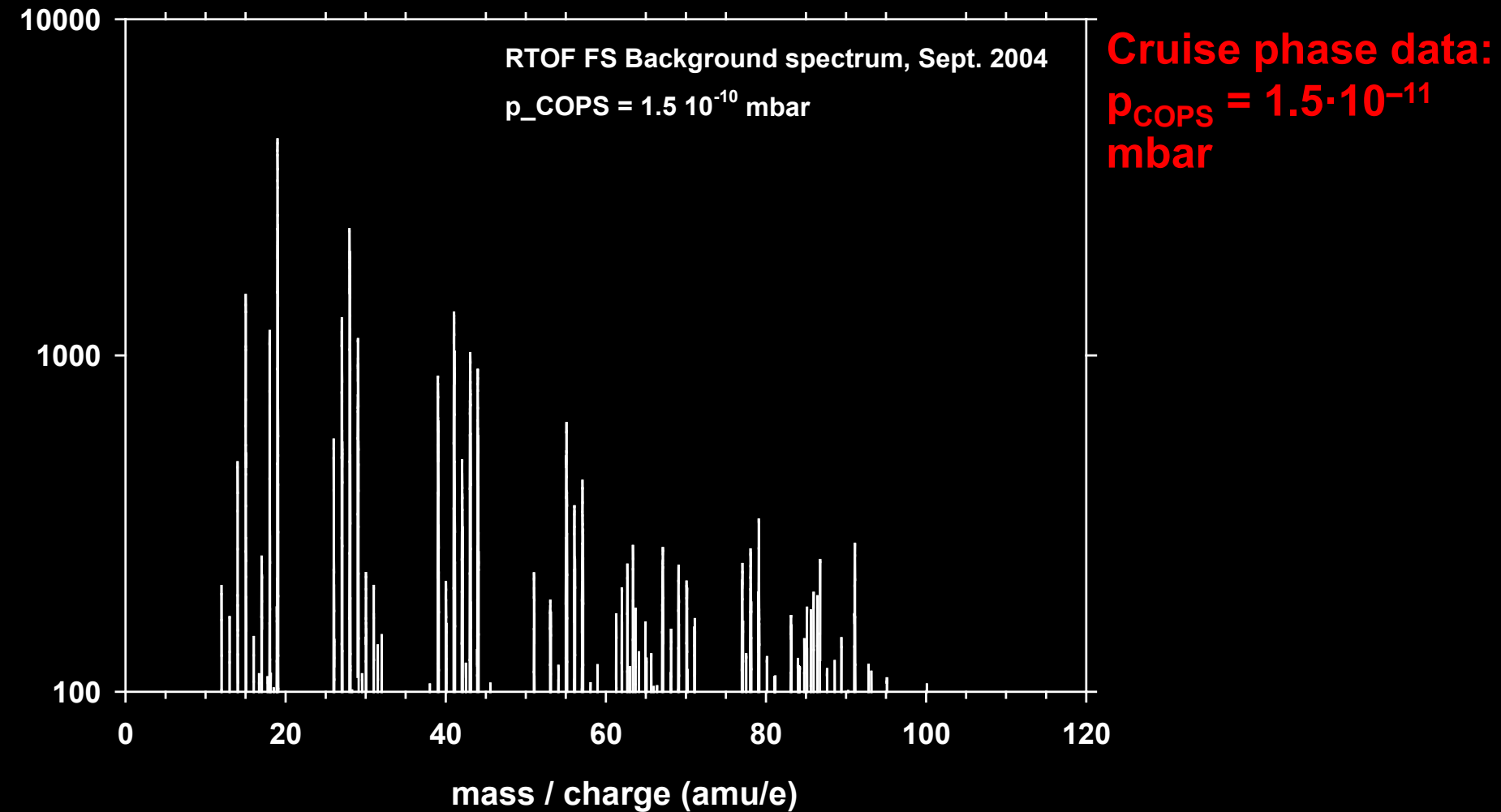


© 1999, Uwe Scherer, (PFTB/NASA Langley Research Center)

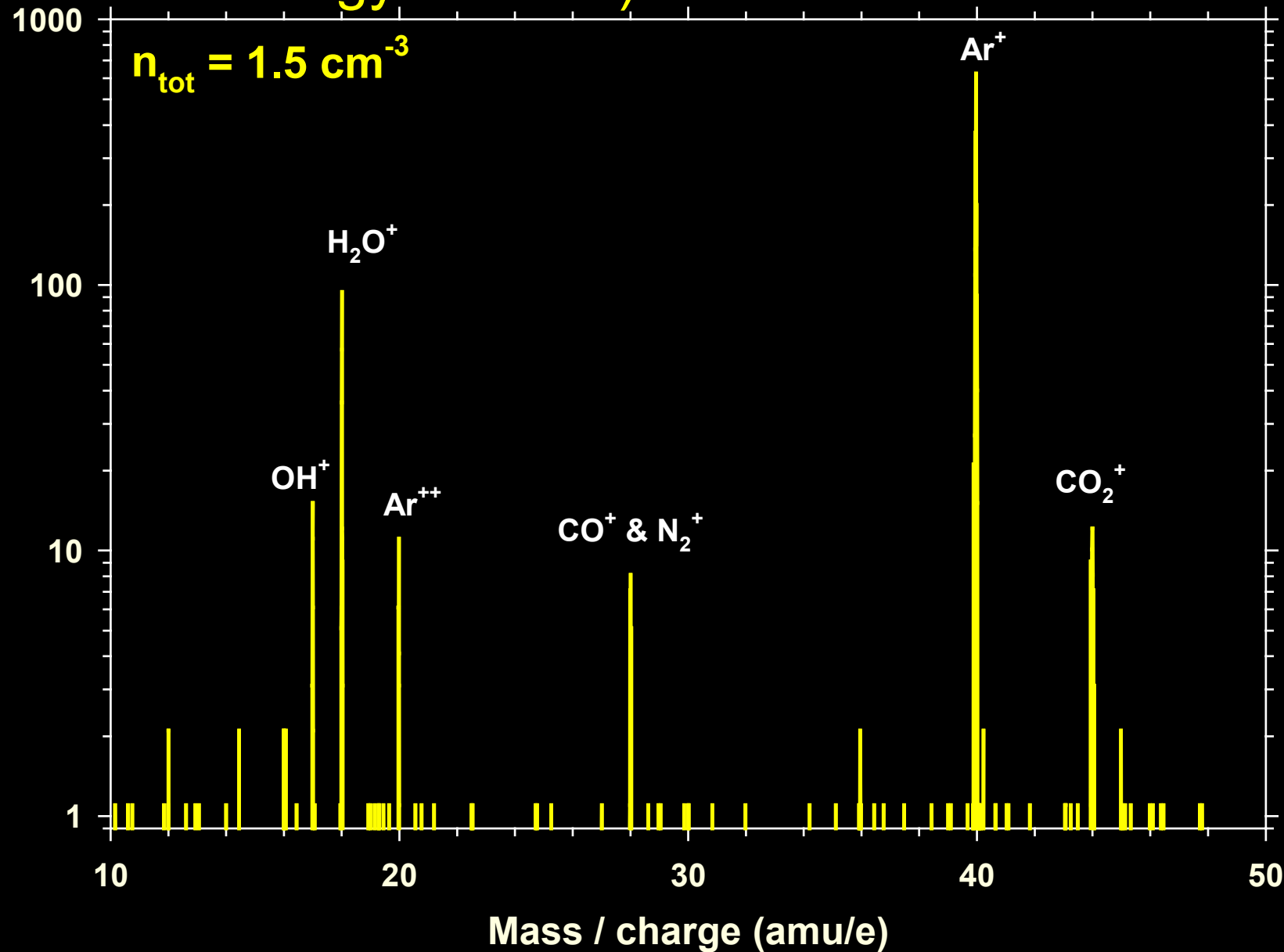
RTOF mass spectrum (prototype) of the calibration compound heptacosafaurotributylamine, a compound to demonstrate mass range. Mass range is unlimited by sensor itself, data acquisition memory however limits the mass range that can be covered. In case of RTOF, the mass range is up to 1000 amu.

S. Scherer, K. Altwegg, H. Balsiger, J. Fischer, A. Jäckel, A. Korth, M. Mildner, D. Piazza, H. Rème, and P. Wurz, "A novel principle for an ion mirror design in time-of-flight mass spectrometry," Int. Jou. Mass Spectr. 251 (2006) 73-81.

RTOF / ROSINA on Rosetta mission



RTOF/ ROSINA ion spectrum Ion energy < 15 eV)



Some identified molecules and fragments in the vicinity of Rosetta S/C

Carbohydrates				PAH		N-H	Hydrazine	C-N	Oxygen	N-O
	C2	C3	C4	C5		N	CN		O	NO
CH	C ₂ H	C ₃ H	C ₄ H	C ₅ H	C ₆ H	NH	CHN	C ₂ H ₂ N	OH	CNO
CH ₂	C ₂ H ₂	C ₃ H ₂	C ₄ H ₂	C ₅ H ₂	C ₆ H ₂	NH ₂	CH ₂ N	C ₂ H ₃ N	OH ₂	HCNO
CH ₃	C ₂ H	C ₃ H ₃	C ₄ H ₃	C ₅ H ₃	C ₆ H ₃	NH ₃	CH ₃ N	C ₂ H ₄ N	ODH	H ₆ CNO
CH ₄	C ₂ H ₄	C ₃ H ₄	C ₄ H ₄	C ₅ H ₄	C ₆ H ₄	N ₂	CH ₃ NH		¹⁸ OH ₂	NO ₂
	C ₂ H ₅	C ₃ H ₅	C ₄ H ₅	C ₅ H ₅	C ₆ H ₅		CH ₃ NH ₂	C ₅ H ₄ N	O ₂	HNO ₂
	C ₂ H ₆	C ₃ H ₆	C ₄ H ₆	C ₅ H ₆		C ₇ H ₆	CH ₃ N ₂ H	C ₅ H ₅ N		H ₄ NO ₂
		C ₃ H ₇	C ₄ H ₇	C ₅ H ₇		C ₇ H ₇	CH ₃ N ₂ H ₂	C ₅ H ₆ N		CHNO ₂
		C ₃ H ₈	C ₄ H ₈	C ₅ H ₈		C ₇ H ₈ Toluene	CH ₃ N ₂ H ₃	C ₅ H ₇ N		CH ₃ NO ₂
			C ₄ H ₉	C ₅ H ₉		C ₈ H ₁₀		C ₅ H ₈ N		CH ₄ NO ₂
			C ₄ H ₁₀	C ₅ H ₁₀		C ₉ H ₁₂				C ₂ H ₆ NO
				C ₅ H ₁₁				C ₄ H ₄ N ₂		H ₂ N ₂ O
				C ₅ H ₁₂						C ₂ N ₂ O
										C ₂ HN ₂ O
										C ₂ H ₂ N ₂ O
										C ₂ H ₃ N ₂ O
										C ₂ H ₅ N ₂ O
										C ₂ H ₆ N ₂ O
										C ₂ H ₇ N ₂ O
										C ₂ H ₈ N ₂ O

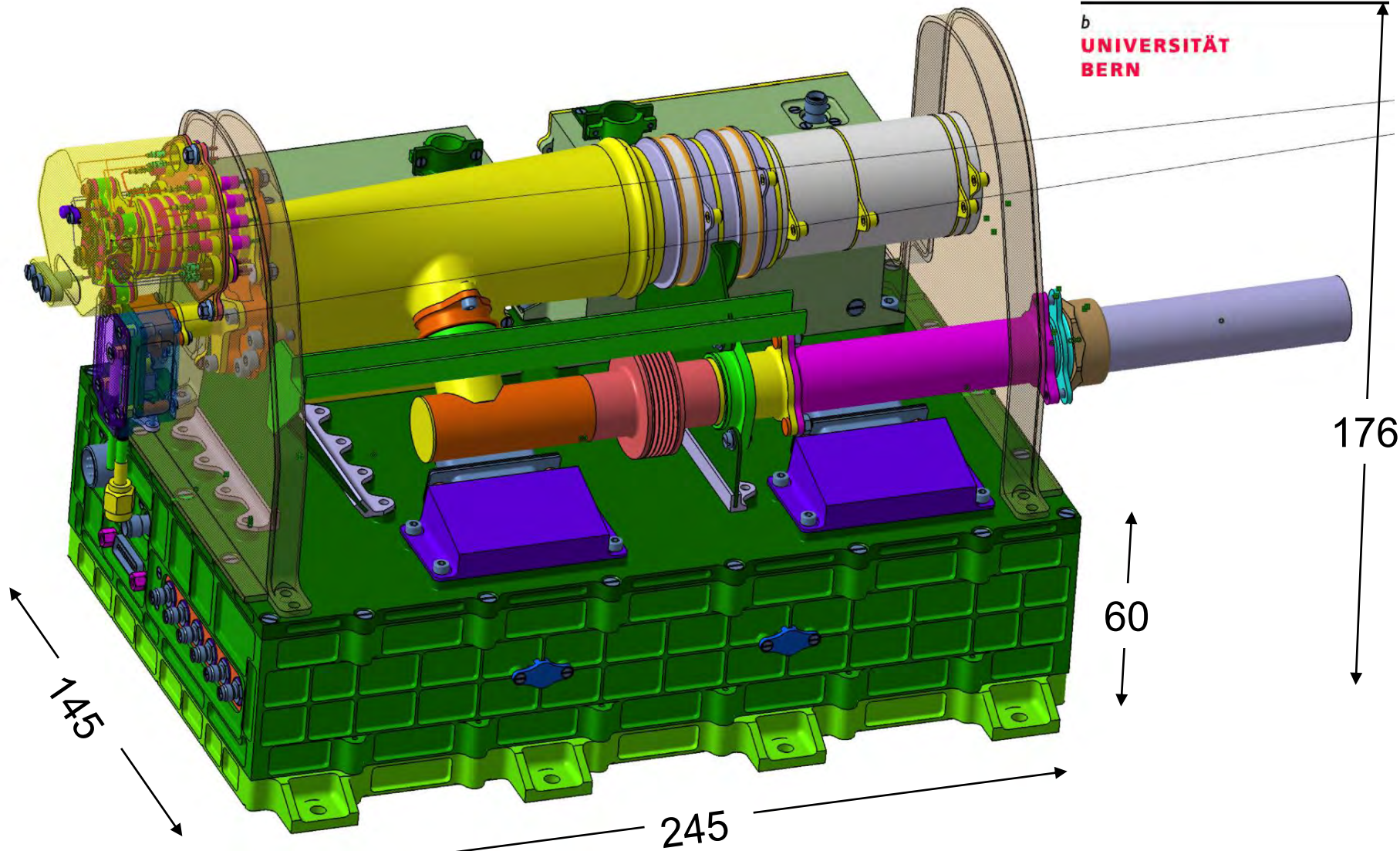
Yellow: Possible fragments from Monomethylhydrazine and N₂O₄

Green: Solvents

Neutral Gas Mass Spectrometer Luna-Resurs / Luna-Glob

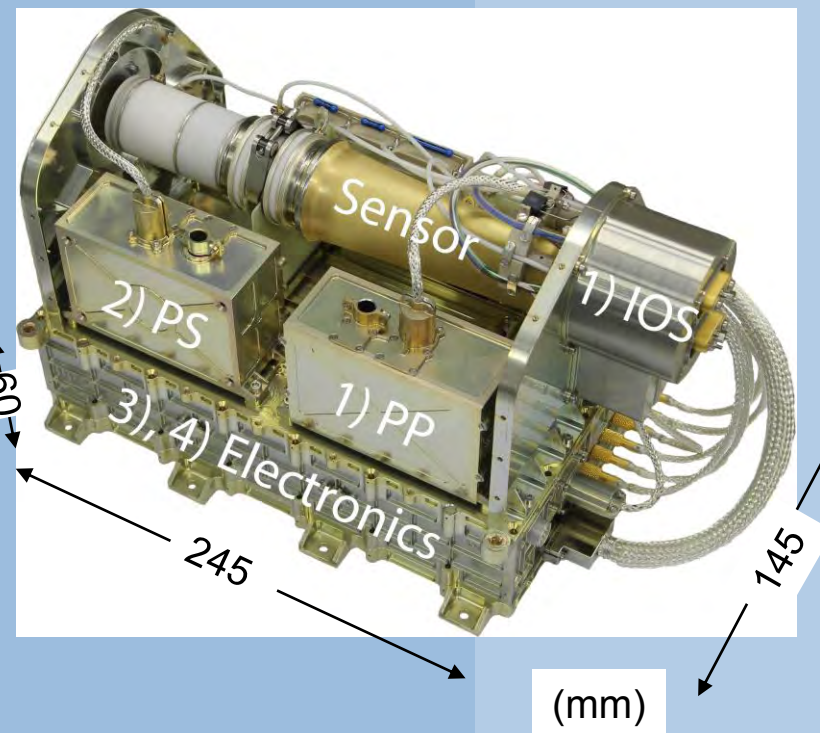
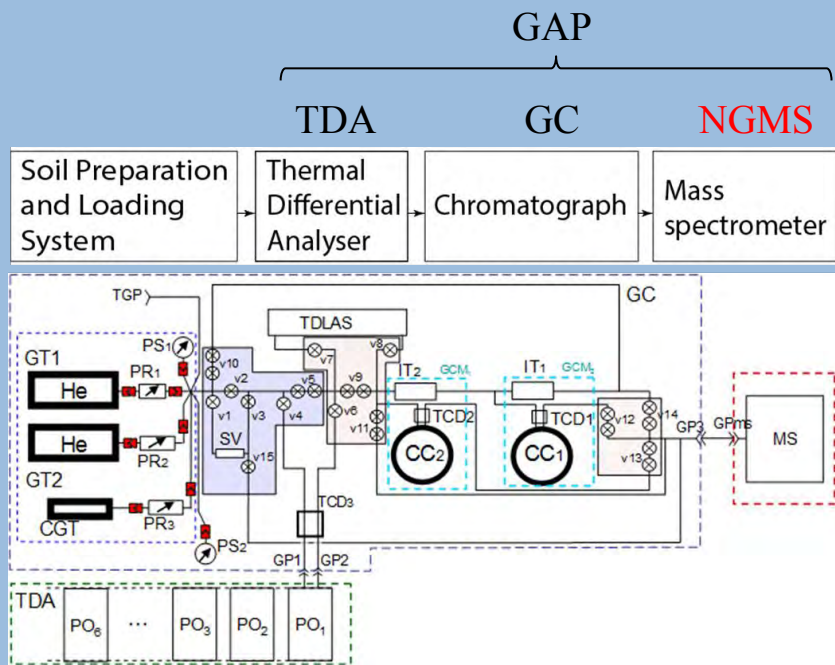
u^b

b
UNIVERSITÄT
BERN



P. Wurz, D. Abplanalp, M. Tulej, and H. Lammer, "A Neutral Gas Mass Spectrometer for the Investigation of Lunar Volatiles," Planet. Sp. Science (2012) in print.

Luna-Resurs Mission: GC – NGMS Complex

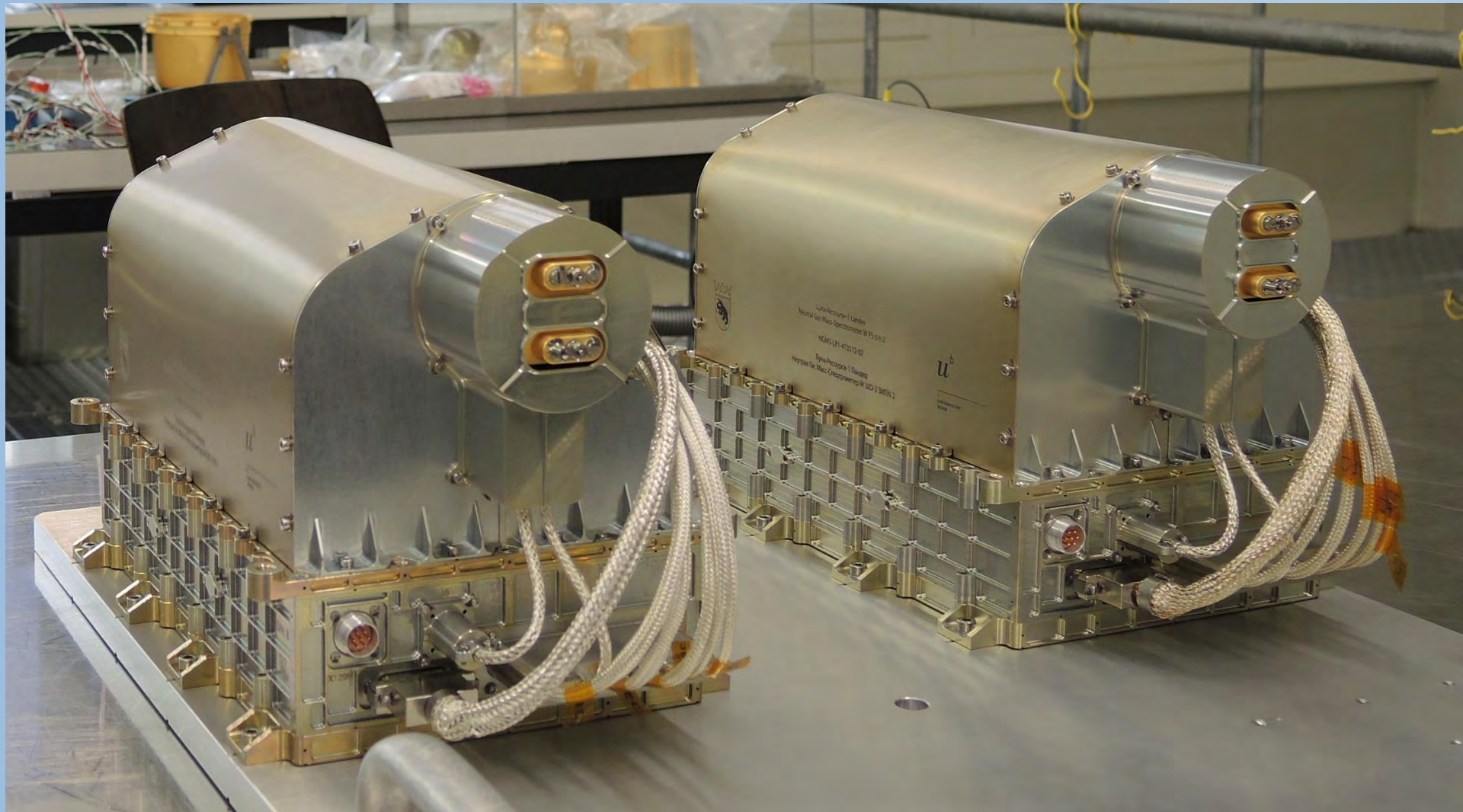


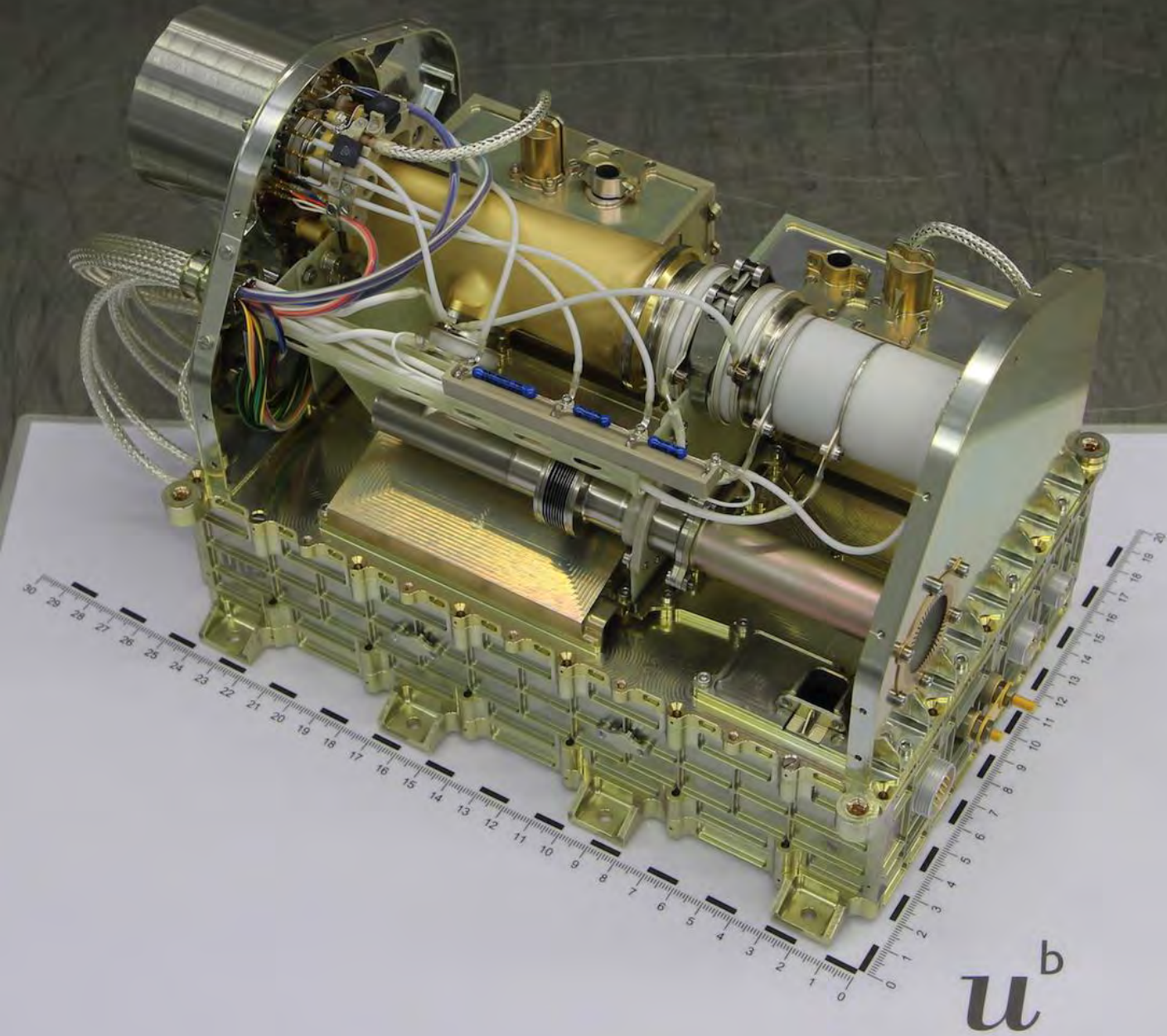
^{1,2} Luna-Resource-1 Lander IRD.
2017.

u^b

b
UNIVERSITÄT
BERN

NGMS / Luna-Resurs GC-MS complex

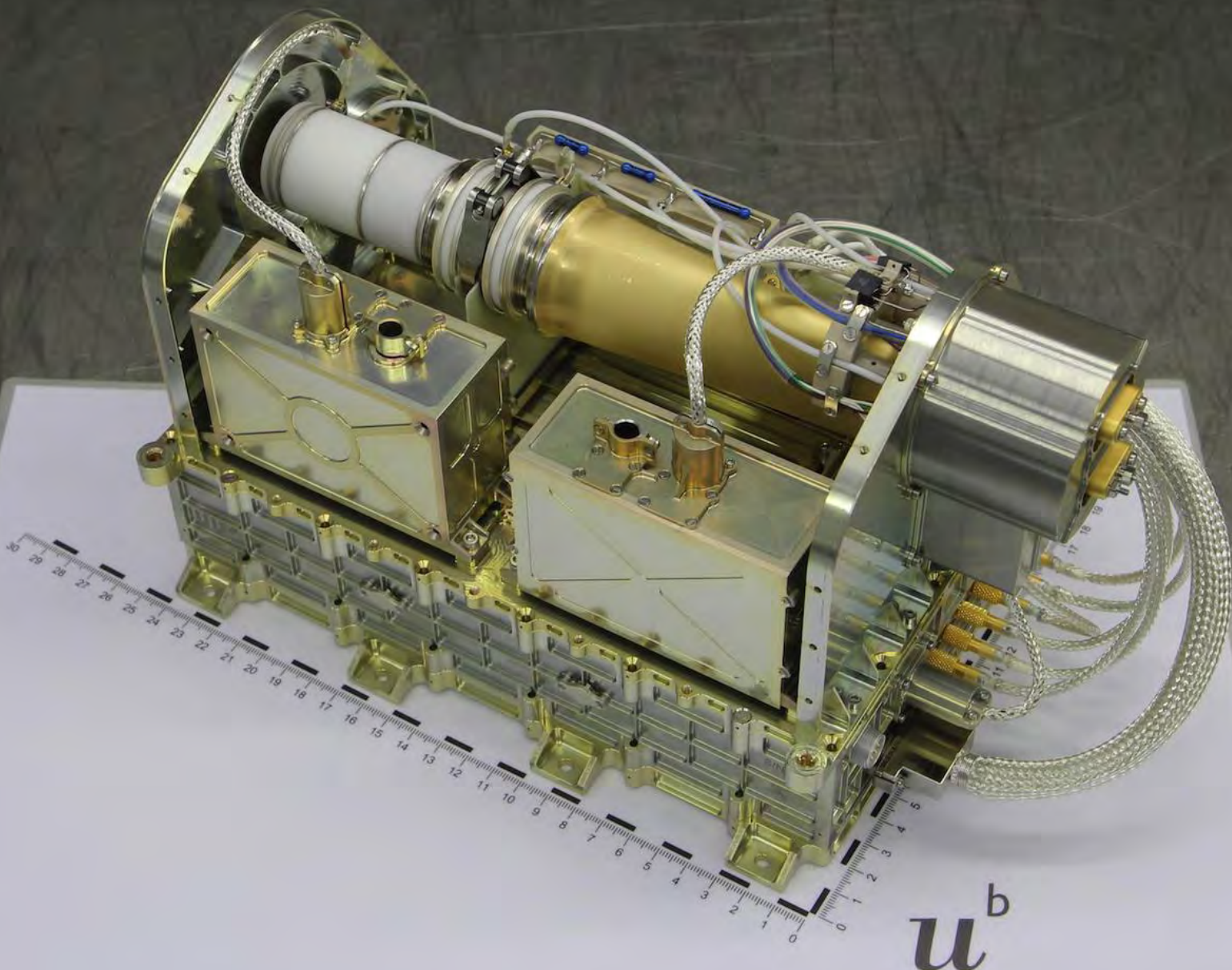




u^b

b

UNIVERSITÄT
BERN



u^b

b

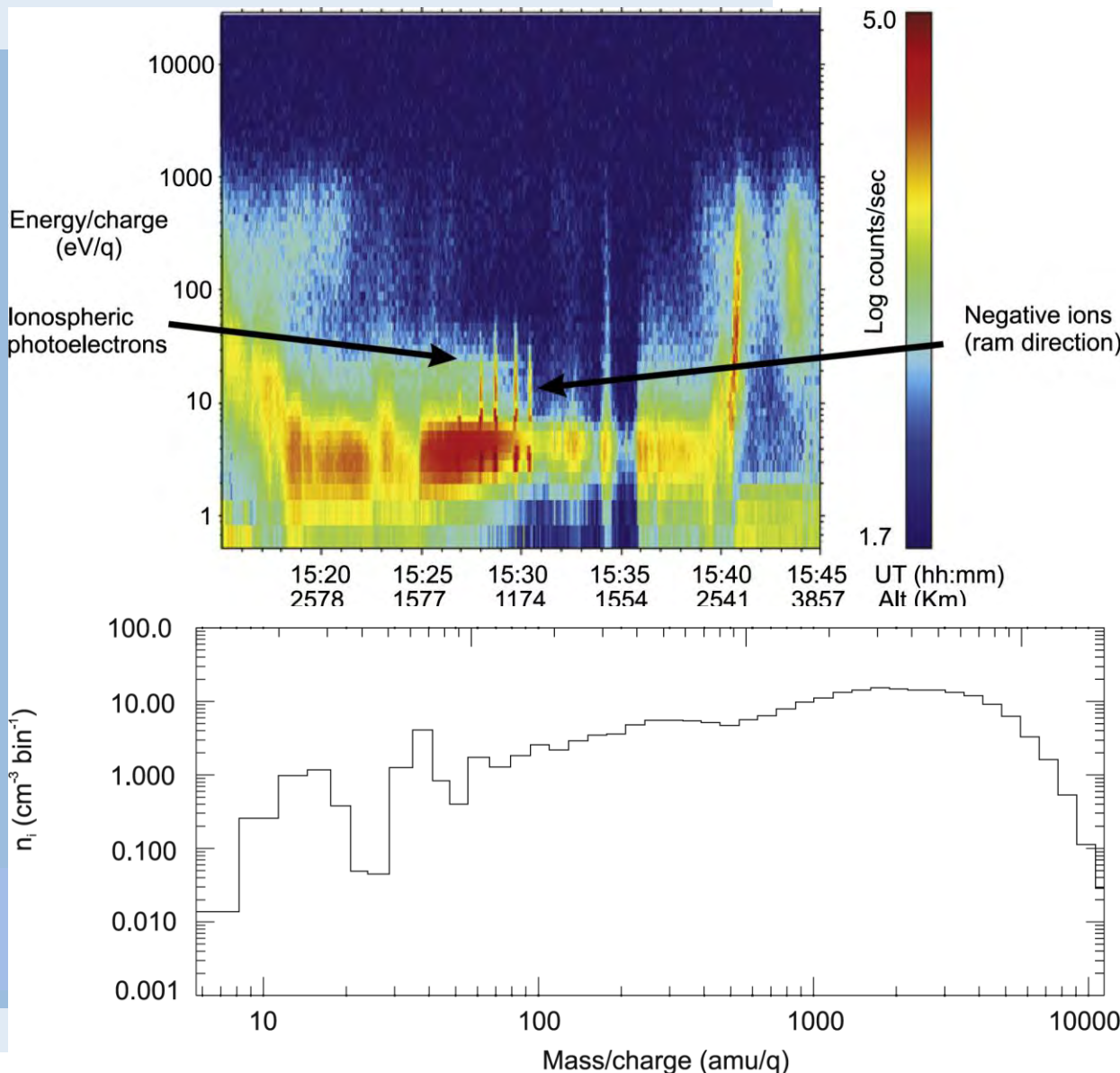
UNIVERSITÄT
BERN

Summary

- ❖ We developed a mass spectrometer for gas analysis of atmospheres and exospheres
 - Mass range 1 – 1000 amu
 - Sensitivity $\approx 1 \text{ cm}^{-3}$ in 10 s integration
 - Prototype successfully used for stratospheric research
 - Abplanalp et al. Adv. Sp. Res. 2010, Wieser et al. Adv. Sp. Res. 2010
 - Flight design for Luna-Resurs
 - Mass 3.5 kg, power 17W
- ❖ Luna-Resurs: GC-MS
 - Investigation of the volatiles contained in the soil by GC-MS analysis
 - Investigation of the lunar exosphere
 - Contamination by spacecraft
 - The Rosetta experience: Schläppi et al. JGR 2010

Negative ions in Titan's Upper Atmosphere

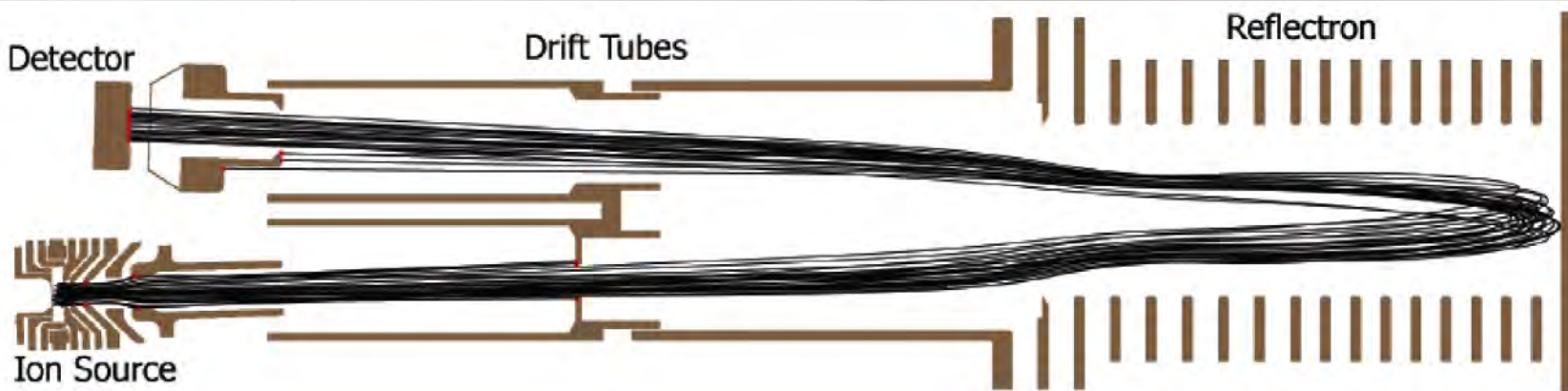
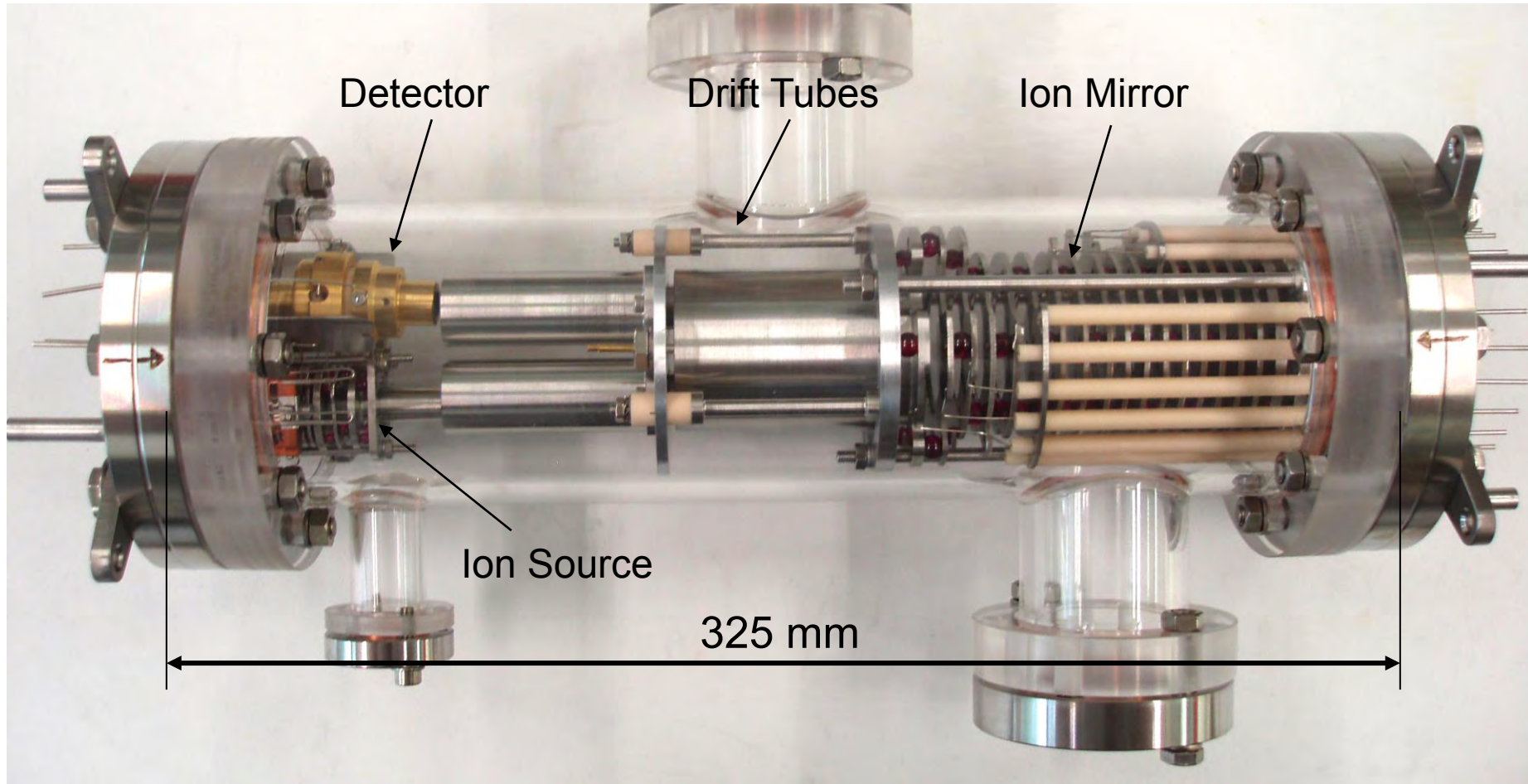
- ❖ Negative ions in the upper atmosphere
- ❖ Typical mass groups
 - M: 10–30, 30–50, 50–80, 80–110, and 110–200 amu
- ❖ Ions with very high masses
 - M < 10'000 amu
- ❖ Important for the formation of organic-rich aerosols (tholins) eventually falling to the surface



A. Coates et al., Geophys.
Res. Lett. 34 (2007) L22103

u^b

b
UNIVERSITÄT
BERN



P-BACE on the MEAP platform



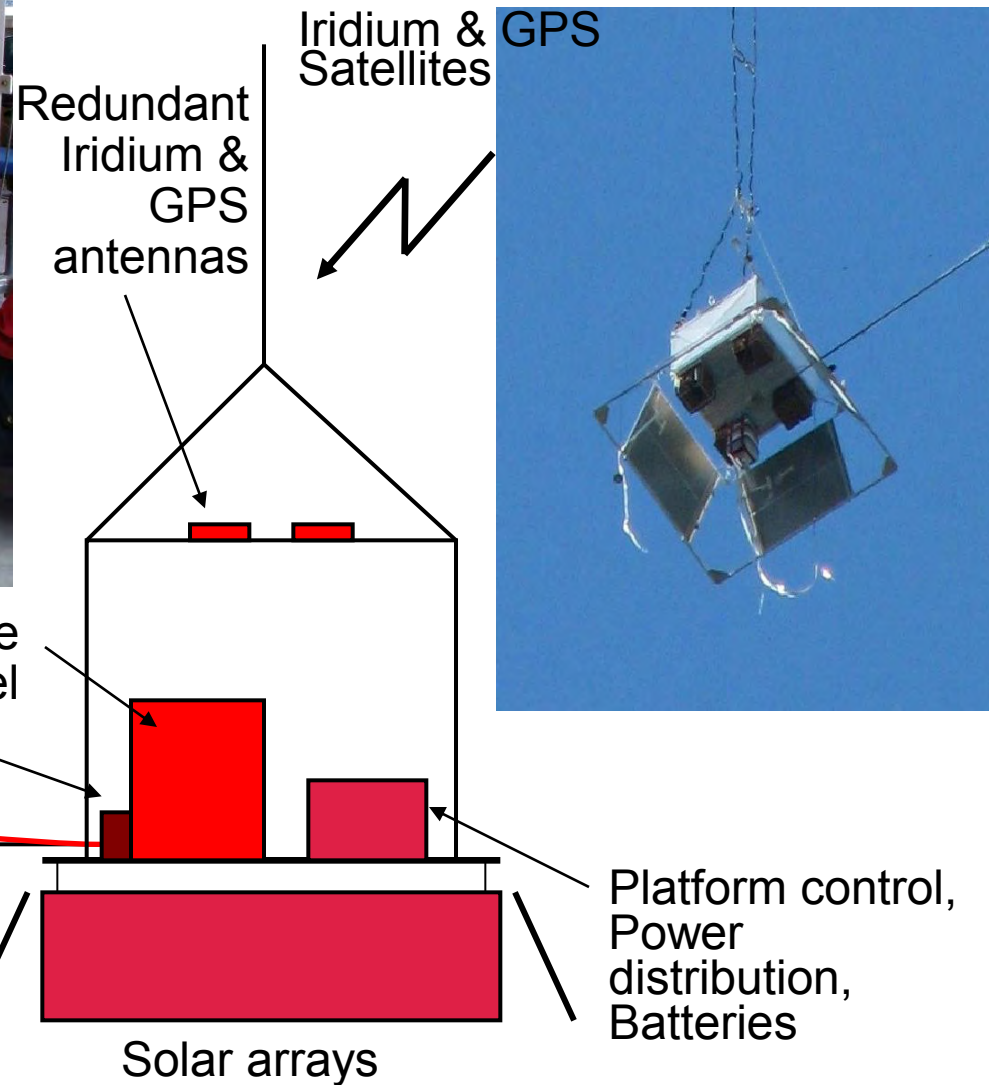
Background image: NASA, <http://visibleearth.nasa.gov/>

- ❖ Balloon provided by Esrange Space Center to test beyond line of sight flight
- ❖ Semicircular flight following the summer polar vortex
- ❖ Launched from Esrange, Sweden, on 28 June 2008
- ❖ Altitude 33 ... 38 km
- ❖ Landed in Canada, near Umingmaktok, on 3 July 2008.
- ❖ Recorded ~ 4500 mass spectra in stratosphere

Species	Measurement 100 spectra (20080701/ 18:50 – 20:40)	Meas. Error [%]	Literature value	Remarks
$^{36}\text{Ar}/^{38}\text{Ar}$	5.313	7	5.35	
$^{36}\text{Ar}/\text{S}_{\text{tot}}$	28 ppm	7	32 ppm	
$^{36}\text{Ar}/^{40}\text{Ar}$	$7.2 \cdot 10^{-4}$	7	$3.38 \cdot 10^{-3}$	Discrimination of small signals (ADC-card)
$^{21}\text{Ne}/\text{S}_{\text{tot}}$	0.053 ppm	21	0.049 ppm	Possible interference with H_2F^+
$^{20}\text{Ne}/^{22}\text{Ne}$	40	80	9.782	Interferences with $^{40}\text{Ar}^{++}$ and CO_2^{++}
$^{78}\text{Kr}/^{84}\text{Kr}$	0.010	50	0.006	
$^{80}\text{Kr}/^{84}\text{Kr}$	0.040	50	0.040	
$^{82}\text{Kr}/^{84}\text{Kr}$	0.200	11	0.203	
$^{83}\text{Kr}/^{84}\text{Kr}$	0.200	11	0.202	
$^{86}\text{Kr}/^{84}\text{Kr}$	0.300	7	0.304	
$\text{Kr}_{\text{tot}}/\text{S}_{\text{tot}}$	1.15 ppm	6	1.14 ppm	
$^{129}\text{Xe}/^{132}\text{Xe}$	0.9615	14	0.9833	
$^{131}\text{Xe}/^{132}\text{Xe}$	0.8846	14	0.7877	
$^{134}\text{Xe}/^{132}\text{Xe}$	0.3462	22	0.3882	
$^{136}\text{Xe}/^{132}\text{Xe}$	0.3077	22	0.3299	
$\text{Xe}_{\text{tot}}/\text{S}_{\text{tot}}$	0.3 ppm	8	0.087 ppm	Consideration of the large cross section for Xe gives a ratio of ~0.08 ppm
$^{196}\text{Hg}/^{202}\text{Hg}$	0.020	82	0.005	
$^{198}\text{Hg}/^{202}\text{Hg}$	0.367	14	0.334	
$^{199}\text{Hg}/^{202}\text{Hg}$	0.600	14	0.565	
$^{200}\text{Hg}/^{202}\text{Hg}$	0.800	14	0.774	
$^{201}\text{Hg}/^{202}\text{Hg}$	0.467	14	0.441	
$^{204}\text{Hg}/^{202}\text{Hg}$	0.233	14	0.230	
$\text{Hg}_{\text{tot}}/\text{S}_{\text{tot}}$	1.72 ppm	6	--	Source unknown (gondola)
$\text{O}_3/\text{S}_{\text{tot}}$	0.59 ppm	21	8 ppm	Pronounced fragmentation
H/D (H ₂ /HD)	8800	14	8694	
$^{23}\text{Na}^+/\text{S}_{\text{tot}}$	0.99 ppm	11	?	Probably oceanic NaCl
$^{40}\text{Ca}^{16}\text{O}_2^+/\text{S}_{\text{tot}}$	0.07 ppm	21	?	Contamination or meteorite material

P. Wurz, D. Abplanalp, M. Tulej, M. Iakovleva, V.A. Fernandes, A. Chumikov, and G. Managadze, "In Situ Mass Spectrometric Analysis in Planetary Science," Sol. Sys. Res. (2012) in press.

P-BACE on the MEAP platform

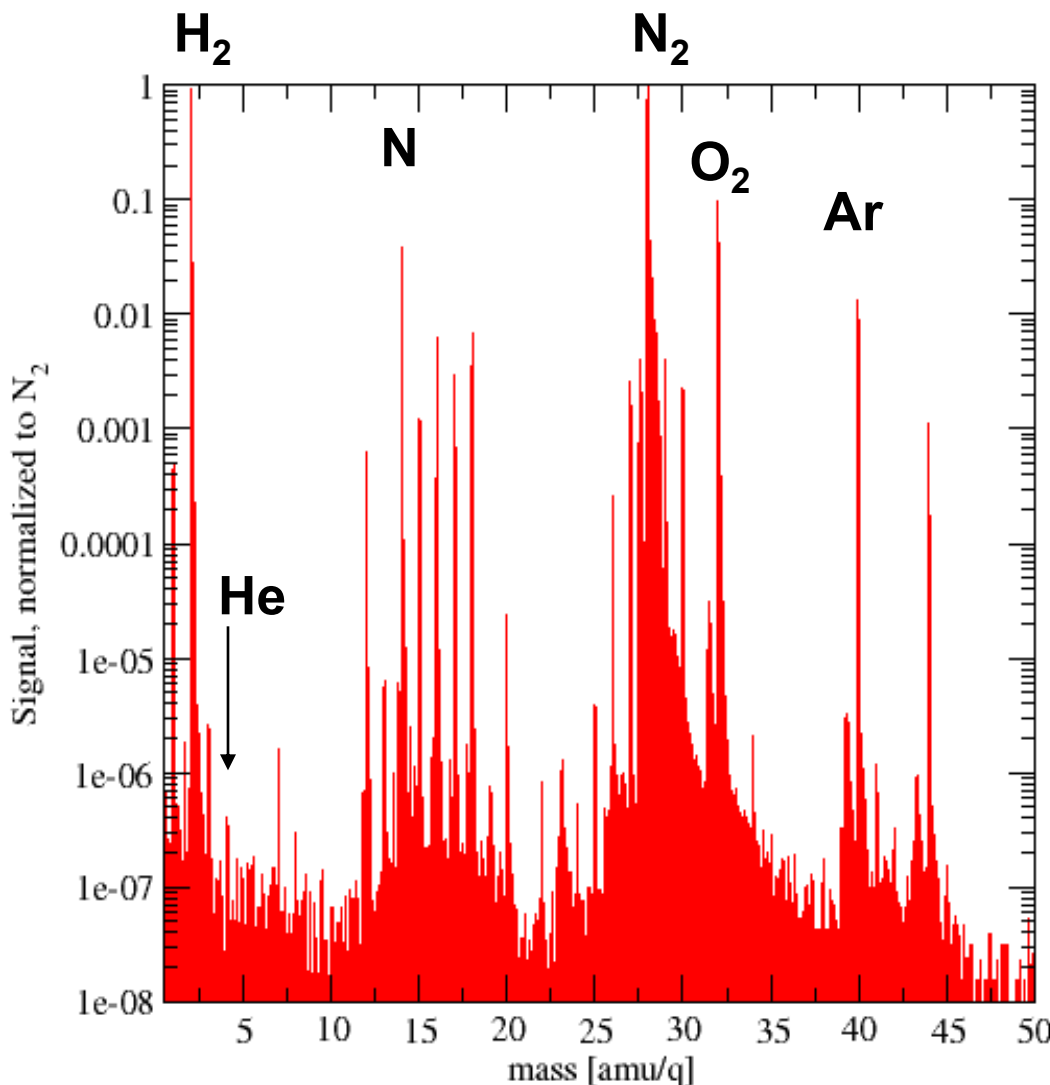


MEAP flight path

- ❖ Balloon provided by Esrange Space Center to test beyond line of sight flight
- ❖ Semicircular flight following the summer polar vortex
- ❖ Launched from Esrange, Sweden on 28 June 2008
- ❖ 116 hours flight time
- ❖ Altitude 33 ... 38 km
- ❖ Landed in Canada, near Umingmaktok, on 3 July 2008.
- ❖ Recorded ~ 4500 mass spectra in stratosphere



P-BACE quicklook data, dynamic range



- ❖ Raw data
- ❖ No background subtracted
- ❖ Dynamic range:
6–7 orders of magnitude per spectrum
- ❖ Mass range:
1–1000 amu/q
- ❖ D. Abplanalp, P. Wurz, L. Huber, I. Leya, E. Kopp, U. Rohner, M. Wieser, L. Kalla, and S. Barabash, Adv. Space Res. 44 (2009) 870–878.

u^b

b
UNIVERSITÄT
BERN

Operations Timeline (Saturn)

Phase	Altitude [km]	Time [min]	Time [sec]	Pressure [mbar]	Speed [m/s]	Integration time [sec]	# Spectra	Vertical resolution [km]	mass spec. [kbit]	total data science [kbit]
	1500	-6.90	-414.18	1.00E-07						
1	450	0	0	1.00E-04	2535.13		10	41.4	25.35	85.15
2	15	2.86	171.6	4.00E+02	2534.97		10	17.2	25.35	85.15
3	14	3.05	183		87.72		5	2.3	0.44	81.95
4	10	3.81	228.6	5.00E+02	87.72		5	9.1	0.44	81.95
5	-13	8.18	490.8	1.60E+03	87.72		5	52.4	0.44	81.95
6	-140	61.4	3684	2.40E+04	39.77		11	290.3	0.44	85.59
								412.7		35066.0
									total data science [Mbit]	34.24

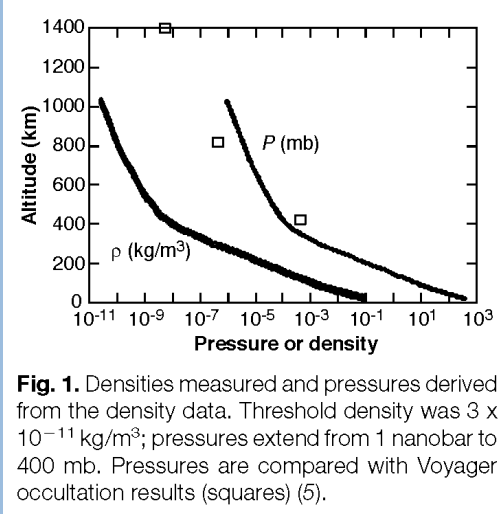


Fig. 1. Densities measured and pressures derived from the density data. Threshold density was $3 \times 10^{-11} \text{ kg/m}^3$; pressures extend from 1 nanobar to 400 mb. Pressures are compared with Voyager occultation results (squares) (5).

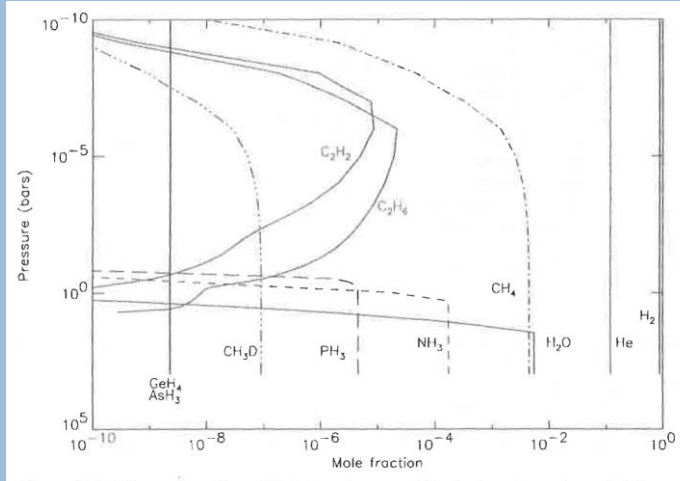


Figure 4.17. Observed and modeled abundance profiles in the atmosphere of Saturn.

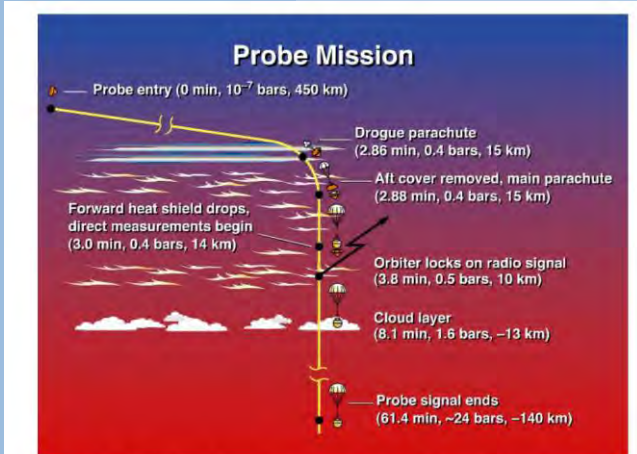


Figure E.1 Galileo entry, descent and deployment sequence shown above will be the basis for the proposed Saturn mission.

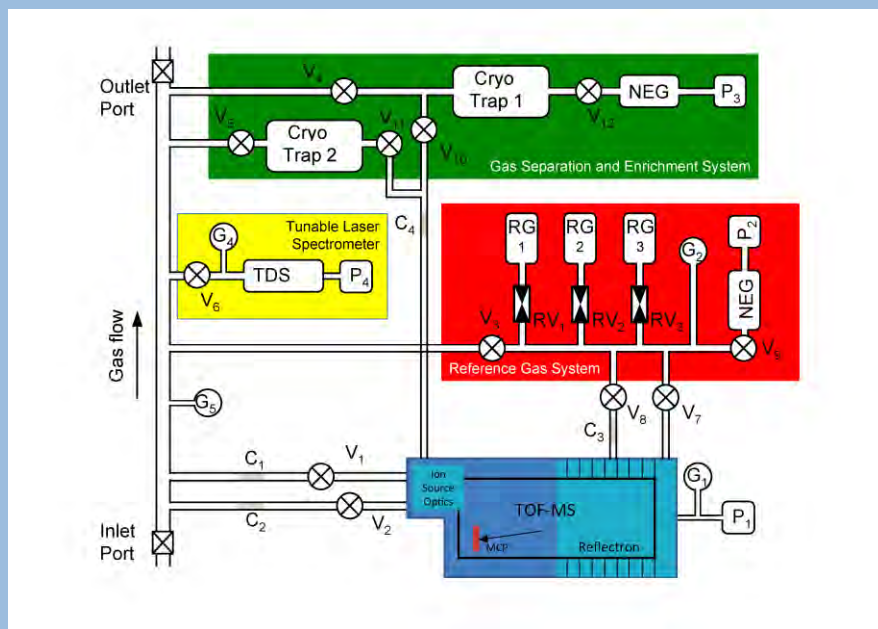
The Hera Mass Spectrometer Experiment

u^b

b
UNIVERSITÄT
BERN

- ❖ Overall System Lead:

- Lead: Peter Wurz (UBE)
- Project Management: Davide Lasi (UBE)
- Lead Engineer: Daniele Piazza (UBE)



- Mass Spectrometer

- Lead: Peter Wurz
- Project Management: Davide Lasi
- Lead Engineer: Daniele Piazza
- Lead Electronics: Matthias Lüthi



- Cryotrap System

- Lead: Hunter Waite (SwRI)
- Project Management: Paul Wilson (SwRI)
- Lead Engineer: Chip Beebe (SwRI)



- Reference Gas System

- Lead: Andrew Morse (OU)
- Project Management: Ross Burgon (OU)
- Lead Engineer: Simon Sheridan (OU)



- TLS System

- Lead:
- Project Management:
- Lead Engineer:



Measurement Accuracies

Phase 1	Accuracy	Phase 2	Accuracy	total [Data Science] [Mbit]	34.24
H ₂ , low Sensitivity	5.0%	H ₂ , low Sensitivity	5.0%		
HD/H ₂	0.9%	HD/H ₂	0.9%		
He, low Sensitivity	5.0%	He, low Sensitivity	5.0%		
³ He/ ⁴ He	1.7%	³ He/ ⁴ He	1.7%		
He/H ₂	1.5%	He/H ₂	1.5%		
CH ₄ , low Sensitivity	5.0%	CH ₄ , low Sensitivity	5.0%		
¹² C/ ¹³ C	1.9%	¹² C/ ¹³ C	1.9%		
H ₂ S, low Sensitivity	5.1%	NH ₃ , low Sensitivity	5.0%		
C ₂ H ₂ , low Sensitivity	9.0%	¹⁴ N/ ¹⁵ N	12.6%		
C ₂ H ₆ , low Sensitivity	8.6%	H ₂ S, low Sensitivity	5.1%		
Ne, low Sensitivity	5.7%	C ₂ H ₂ , low Sensitivity	9.0%		
Ar, low Sensitivity	5.0%	C ₂ H ₆ , low Sensitivity	8.6%		
Kr, low Sensitivity	12.1%	Ne, low Sensitivity	5.7%		
Xe, low Sensitivity	41.8%	Ar, low Sensitivity	5.0%		
		Kr, low Sensitivity	12.1%		
		Xe, low Sensitivity	41.8%		
Phase 3/4/5	Accuracy	Phase 6	Accuracy	Noble gases (3 times Cryotrap)	Accuracy
CH ₄ , high Sensitivity	5.0%	CH ₄ , high Sensitivity	5.0%	Ar Enriched	
¹² C/ ¹³ C	0.3%	¹² C/ ¹³ C	0.2%		36Ar/38Ar 0.10%
NH ₃ , high Sensitivity	5.0%	NH ₃ , high Sensitivity	5.0%	Kr Enriched	
¹⁴ N/ ¹⁵ N	1.5%	¹⁴ N/ ¹⁵ N	12.0%		78Kr/Kr_tot 1.06%
H ₂ O at 1 bar, high Sensitivity	6.5%	H ₂ O at 10 bar, high Sensitivity	5.0%		80Kr/Kr_tot 1.13%
H ₂ S, high Sensitivity	5.0%	¹⁶ O/ ¹⁷ O	7.4%		82Kr/Kr_tot 0.46%
CO, high Sensitivity	163.8%	¹⁶ O/ ¹⁸ O	3.1%		83Kr/Kr_tot 0.28%
CO ₂ , high Sensitivity	457.7%	H ₂ S, high Sensitivity	5.0%		84Kr/Kr_tot 0.23%
PH ₃ at 1 bar, high Sensitivity	5.1%	CO, high Sensitivity	110.5%		86Kr/Kr_tot 0.21%
A ₃ H, high Sensitivity	69.2%	CO ₂ , high Sensitivity	308.6%	Xe Enriched	
GeH ₄ , high Sensitivity	445.0%	PH ₃ , high Sensitivity	5.0%		124Xe/Xe_tot 6.18%
C ₂ H ₂ , high Sensitivity	5.1%	A ₃ H, high Sensitivity	46.8%		126Xe/Xe_tot 8.74%
C ₂ H ₆ , high Sensitivity	5.1%	GeH ₄ , high Sensitivity	300.0%		128Xe/Xe_tot 6.28%
Ne, high Sensitivity	5.0%	C ₂ H ₂ , high Sensitivity	5.0%		129Xe/Xe_tot 1.19%
Ar, high Sensitivity	5.0%	C ₂ H ₆ , high Sensitivity	5.0%		130Xe/Xe_tot 0.85%
Kr, high Sensitivity	5.2%	Ne, high Sensitivity	5.0%		131Xe/Xe_tot 0.87%
Xe, high Sensitivity	6.1%	²⁰ Ne/ ²¹ Ne	5.4%		132Xe/Xe_tot 0.49%
		²¹ Ne/ ²² Ne	5.4%		134Xe/Xe_tot 0.60%
		Ar, high Sensitivity	5.0%		136Xe/Xe_tot 0.74%
		Kr, high Sensitivity	5.1%		
		Xe, high Sensitivity	5.5%		

Operations Timeline (old)

Descent Time [min]	Pressure [mbar]	Measurement campaign	Add. activity
-178 to -143	10^{-6} to 10^{-3}	Mass spectra, low sens. (incl. H ₂ /He)	Collect hydro carbons
-142	10^{-3}	Hydro carbons measurements from trap	
-141 to -90	10^{-3} to 10^{-1}	Mass spectra, low sens. (incl. H ₂ /He)	Collect hydro carbons
-89	10^{-1}	Hydro carbons measurements from trap	
-88 to -55	10^{-1} to 10	Mass spectra, high sens.	Collect hydro carbons
-55	10	Hydro carbons measurements from trap	
-54 to -35	10 to 100	Mass spectra, high sens.	Collect noble gases
-35	100	Noble gas measurements from trap	
-35 to -17	100 to 1000	Mass spectra, high sens.	Collect noble gases
-17	1000	Noble gas measurements from trap	
-17 to -2.5	1000 to 8000	Mass spectra, high sens.	Collect noble gases
-2.5	8000	Noble gas measurements from trap	
-2.5 to 0	8000 to 10'000	Mass spectra, high sens.	
0 to +6	10'000 to 20'000	Mass spectra, high sens.	

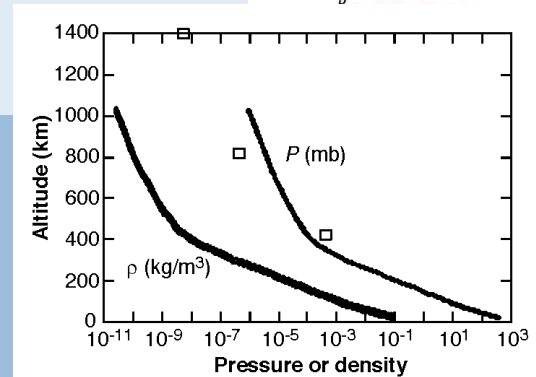


Fig. 1. Densities measured and pressures derived from the density data. Threshold density was $3 \times 10^{-11} \text{ kg}/\text{m}^3$; pressures extend from 1 nanobar to 400 mb. Pressures are compared with Voyager occultation results (squares) (5).

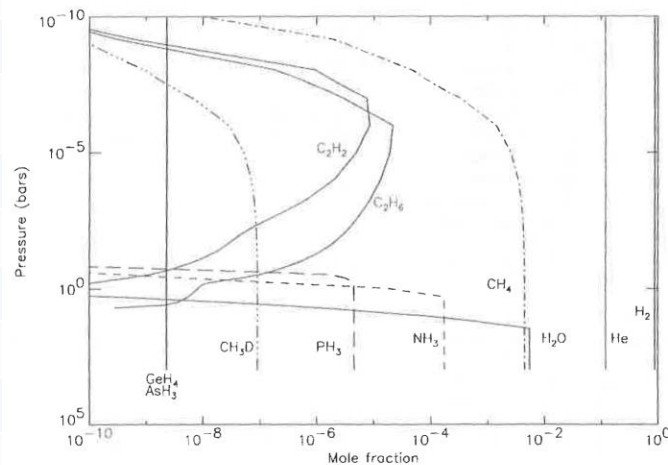


Figure 4.17. Observed and modeled abundance profiles in the atmosphere of Saturn.

Measurement Accuracies: Known Species

Objective	Measurement mode	Accuracy for 50 s integration
H ₂	low sensitivity	5%
He	low sensitivity	5%
He/H ₂	low sensitivity	2.1%
CH ₄	low sensitivity	5%
NH ₃	low sensitivity	5%
¹⁴ N/ ¹⁵ N from NH ₃	low sensitivity	5.6%
H ₂ S	low sensitivity	5%
C ₂ H ₂	low sensitivity	6%
C ₂ H ₆	low sensitivity	5.9%
PH ₃	low sensitivity	5.6%
H ₂ O at 2 bar	high sensitivity	5.2%
H ₂ O at 10 bar	high sensitivity	5%
¹⁶ O/ ¹⁷ O in H ₂ O	high sensitivity	2.4%
¹⁶ O/ ¹⁸ O in H ₂ O	high sensitivity	1%
CO	high sensitivity	52%
CO ₂	high sensitivity	150%
AsH ₃	high sensitivity	22%
GeH ₄	high sensitivity	140%

Measurement Accuracies: Noble Gases

Objective	Measurement mode	Accuracy for 50 s integration	Objective	Measurement mode	Accuracy for 50 s integration
³ He/ ⁴ He	Low sensitivity	0.8%	Xe	Low / high sensitivity	19% / 5.1%
Ne	Low / high sensitivity	5.2% / 5%	¹²⁴ Xe/Xe_tot	Cryotrap	6.2%
²⁰ Ne/ ²¹ Ne	High sensitivity	2.5%	¹²⁶ Xe/Xe_tot	Cryotrap	8.8%
²¹ Ne/ ²² Ne	High sensitivity	2.6%	¹²⁸ Xe/Xe_tot	Cryotrap	6.3%
Ar	Low sensitivity	5%	¹²⁹ Xe/Xe_tot	Cryotrap	1.2%
³⁶ Ar/ ³⁸ Ar	Cryotrap	0.11%	¹³⁰ Xe/Xe_tot	Cryotrap	0.86%
Kr	Low / high sensitivity	7% / 5%	¹³¹ Xe/Xe_tot	Cryotrap	0.87%
⁷⁸ Kr/Kr_tot	Cryotrap	1.1%	¹³² Xe/Xe_tot	Cryotrap	0.49%
⁸⁰ Kr/Kr_tot	Cryotrap	1.1%	¹³⁴ Xe/Xe_tot	Cryotrap	0.6%
⁸² Kr/Kr_tot	Cryotrap	0.46%	¹³⁶ Xe/Xe_tot	Cryotrap	0.74%
⁸³ Kr/Kr_tot	Cryotrap	0.28%			
⁸⁴ Kr/Kr_tot	Cryotrap	0.23%			
⁸⁶ Kr/Kr_tot	Cryotrap	0.21%			

Summary

Possible Implementation

- ❖ Atmospheric composition complex
 - Mass spectrometer
 - Enrichment cells, e.g. Cryo trap
 - Chemical pre-separation
 - TLS, He/H
- ❖ Sufficient sensitivity and vertical resolution
 - Non-scanning instruments → Time of Flight instrument
- ❖ Mass resolution and mass range
 - Not critical
 - Several mass analyser options
- ❖ Limit complexity
 - Simple Time of Flight instrument
 - Traps
 - Chemical pre-separation
- ❖ Limit instrument resources
 - ❖ Two mass spectrometers ?
 - ❖ One MS for survey mode
 - Full mass spectra
 - High cadence during entire descent
 - ❖ One MS dedicated for specific objectives
 - Noble gases, with traps
 - High mass resolution
 - Aerosols

u^b

b
UNIVERSITÄT
BERN

Micro-Gas Chromatography Systems

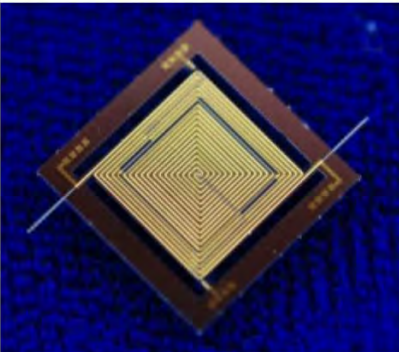
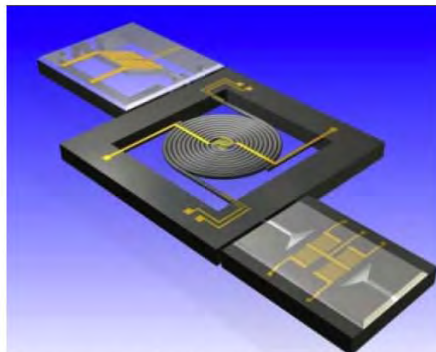


Figure 1: Left: Drawing of complete μ GC analysis system. Right: A 25cm-long separation column with built-in fluidic interconnects.

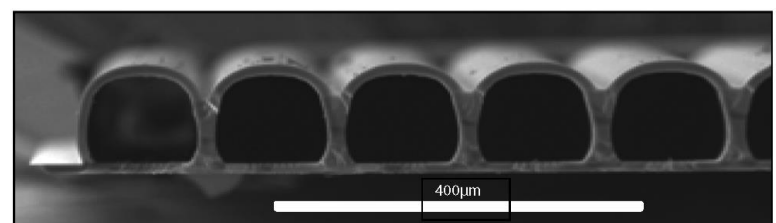
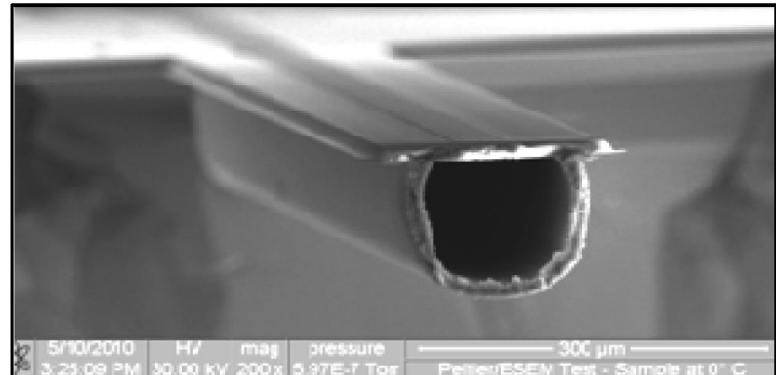


Figure 3: Cross-sections of the laser-cut fluidic interconnects and the column cross-section. The flow channel is 120 μ m across and 90 μ m deep.

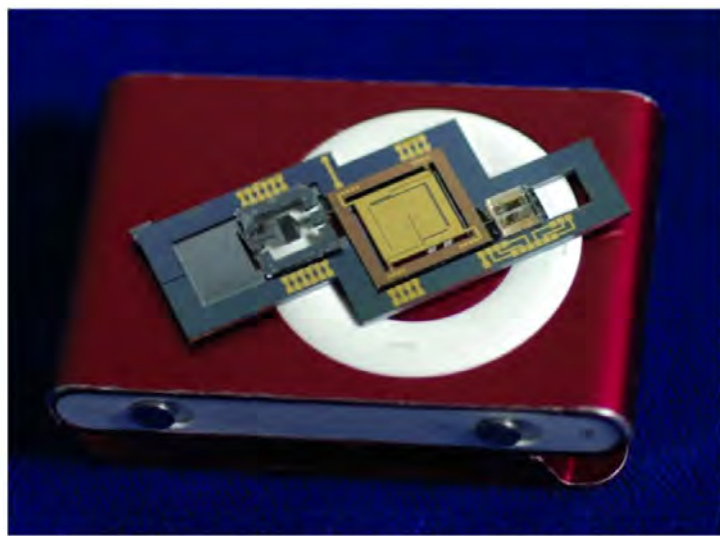


Figure 9: A 25cm separation column, single-bed preconcentrator, and chemi-resistive detector on a 2nd generation Apple iPod Shuffle about the size of the intended μ GC system. The outer circle is about the size of a U.S. quarter.

K.T.M. Beach, S.M. Reidy, R.J.M. Gordenker, and K.D. Wise, A low-mass high-speed μ GC separation column with built-in fluidic chip-to-chip interconnects, IEEE proc. 2011

u^b

b
UNIVERSITÄT
BERN

Quadrupole Ion Trap Mass Spectrometer

2158 Rev. Sci. Instrum., Vol. 73, No. 5, May 2002

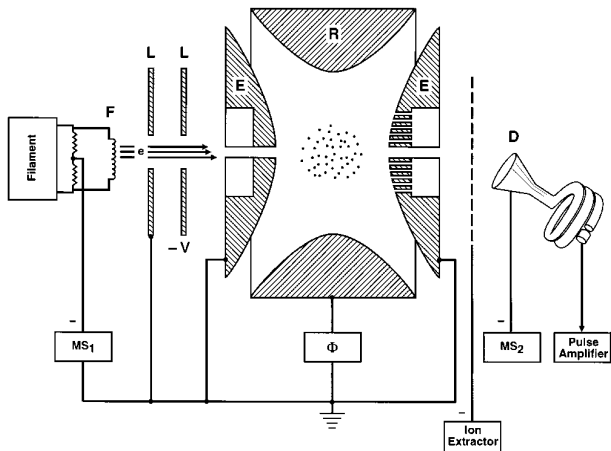


FIG. 1. Schematic diagram of the Paul ion trap and electronics. The electron filament is denoted by F ; the pulser which switches the filament bias voltage is MS_1 ; that for switching the high voltage to the ion detector is MS_2 ; the electron e lens elements are L ; the trap end caps are E ; the trap ring is R ; and the detector is D . Timing sequences of the voltages F , D , and Φ are given in Fig. 2.

O. J. Orient and A. Chutjiana, A compact, high-resolution Paul ion trap mass spectrometer with electron-impact ionization, Review of Scientific Instruments 73, 2157 (2002)

ELECTRON GUN

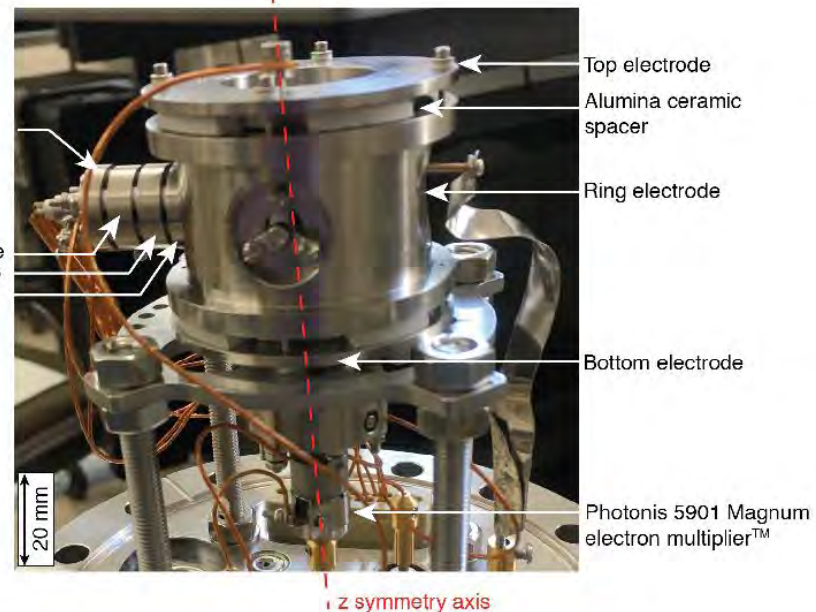
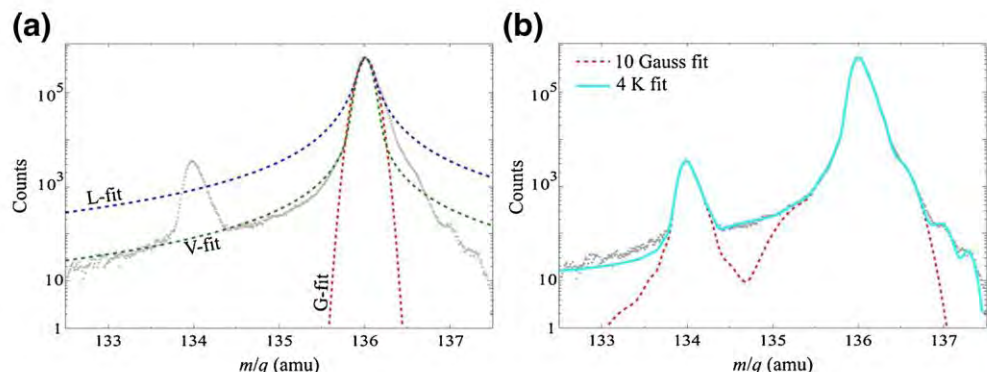


Fig. 1: Picture of the side-ionization JPL-QITMS



Orbitrap

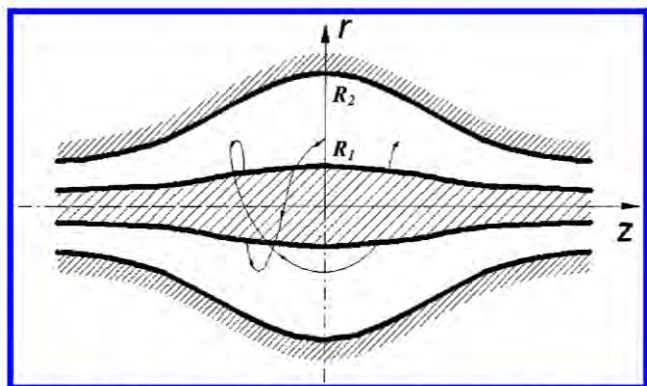


Figure 1. Equipotentials of the quadro-logarithmic field and an example of a stable ion trajectory

$$U(r,z) = \frac{k}{2} \left(z^2 - \frac{r^2}{2} \right) + \frac{k}{2} (R_m)^2 \ln \left[\frac{r}{R_m} \right] + C$$

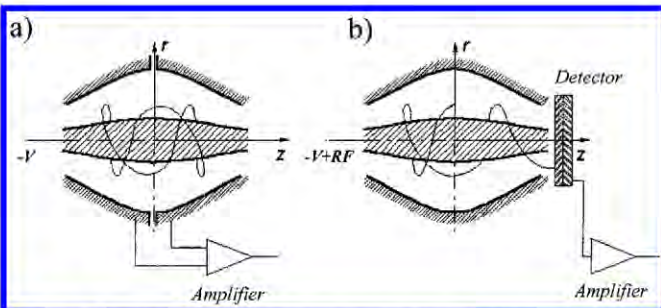


Figure 2. Modes of mass analysis in the orbitrap: (a) Fourier transform mass spectrometry (image current detection); (b) mass-selective instability (detection using secondary electron multiplier).

❖ Early work

- A. Makarov, Electrostatic axially harmonic orbital trapping: a highperformance technique of mass analysis. *Anal. Chem.* 72, (2000) 1156–1162
- Qizhi Hu, Robert J. Noll, Hongyan Li, Alexander Makarov, Mark Hardman, and R. Graham Cooks, The Orbitrap: a new mass spectrometer, *J. Mass Spectrom.* 2005; 40: 430–443

❖ Theory

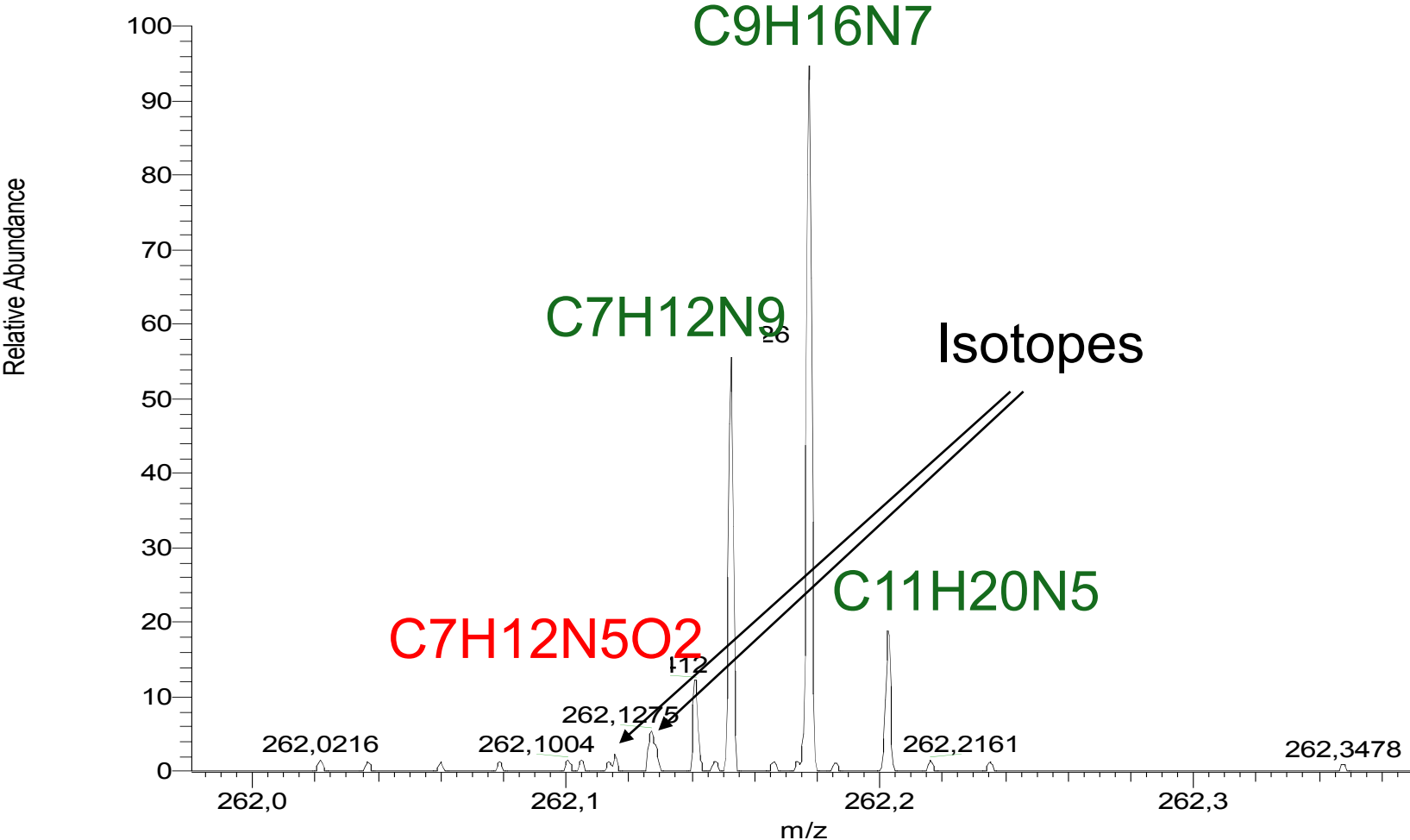
- Andriy Kharchenko, Gleb Vladimirov, Ron M. A. Heeren, Eugene N. Nikolaev, Performance of Orbitrap Mass Analyzer at Various Space Charge and Non-Ideal Field Conditions: Simulation Approach, *J. Am. Soc. Mass Spectrom.* (2012) 23:977–987

❖ Multiple MS (MS^M)

- Robert Cho, Yingying Huang, Jae C. Schwartz, Yan Chen, Timothy J. Carlson, Ji Ma, MS^M , an Efficient Workflow for Metabolite Identification Using Hybrid Linear Ion Trap Orbitrap Mass Spectrometer, *J. Am. Soc. Mass Spectrom.* (2012) 23:880–888

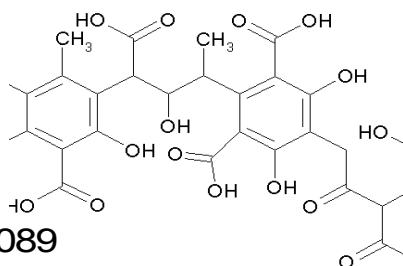
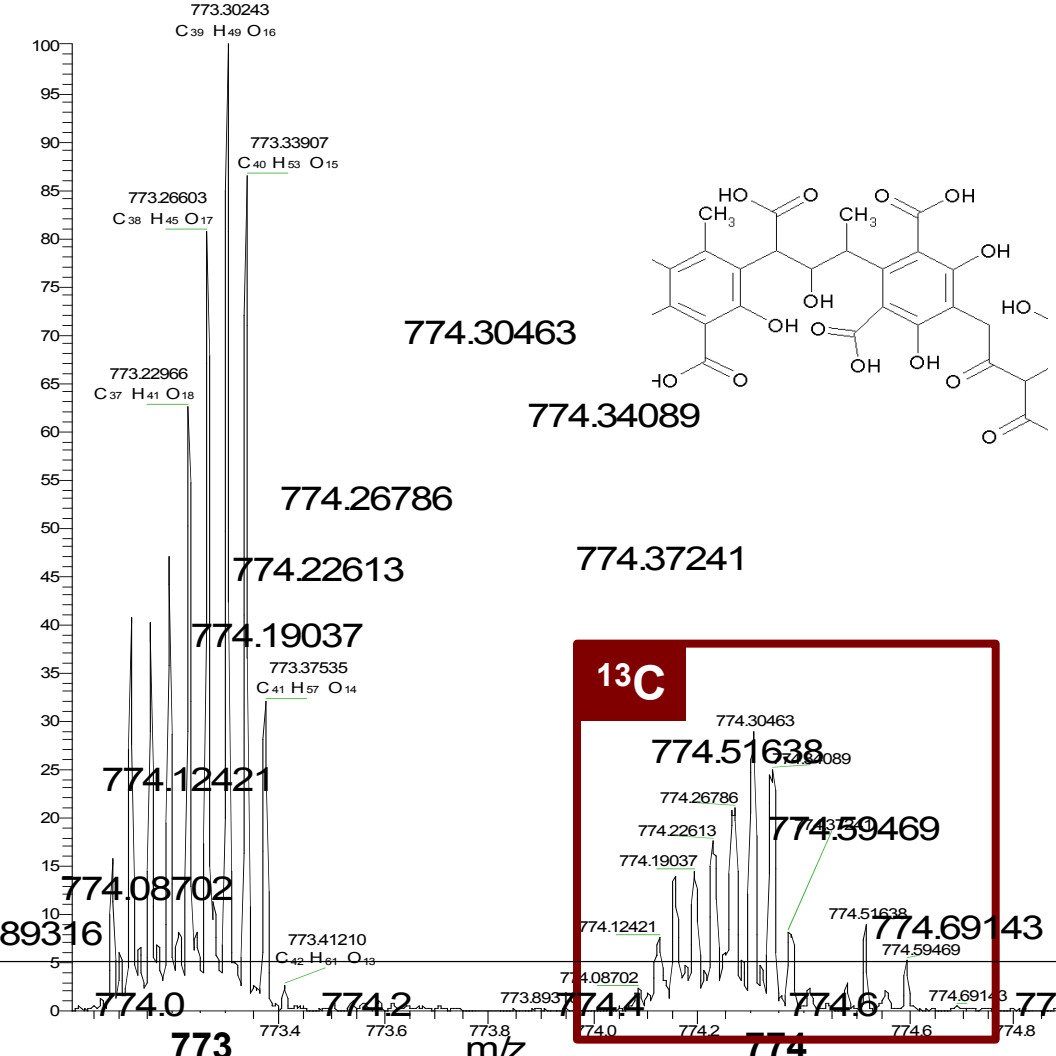
Zoom on mass 262

070511_Lot1MeOH_b #663-697 RT: 19,32-20,28 AV: 35 NL: 1,02E5
T: FTMS + p ESI Full ms [50,00-500,00]

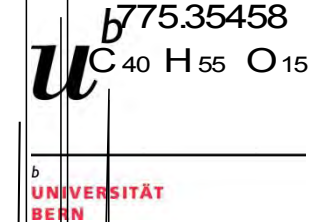


Isotopic abundances, example on complex mixture...

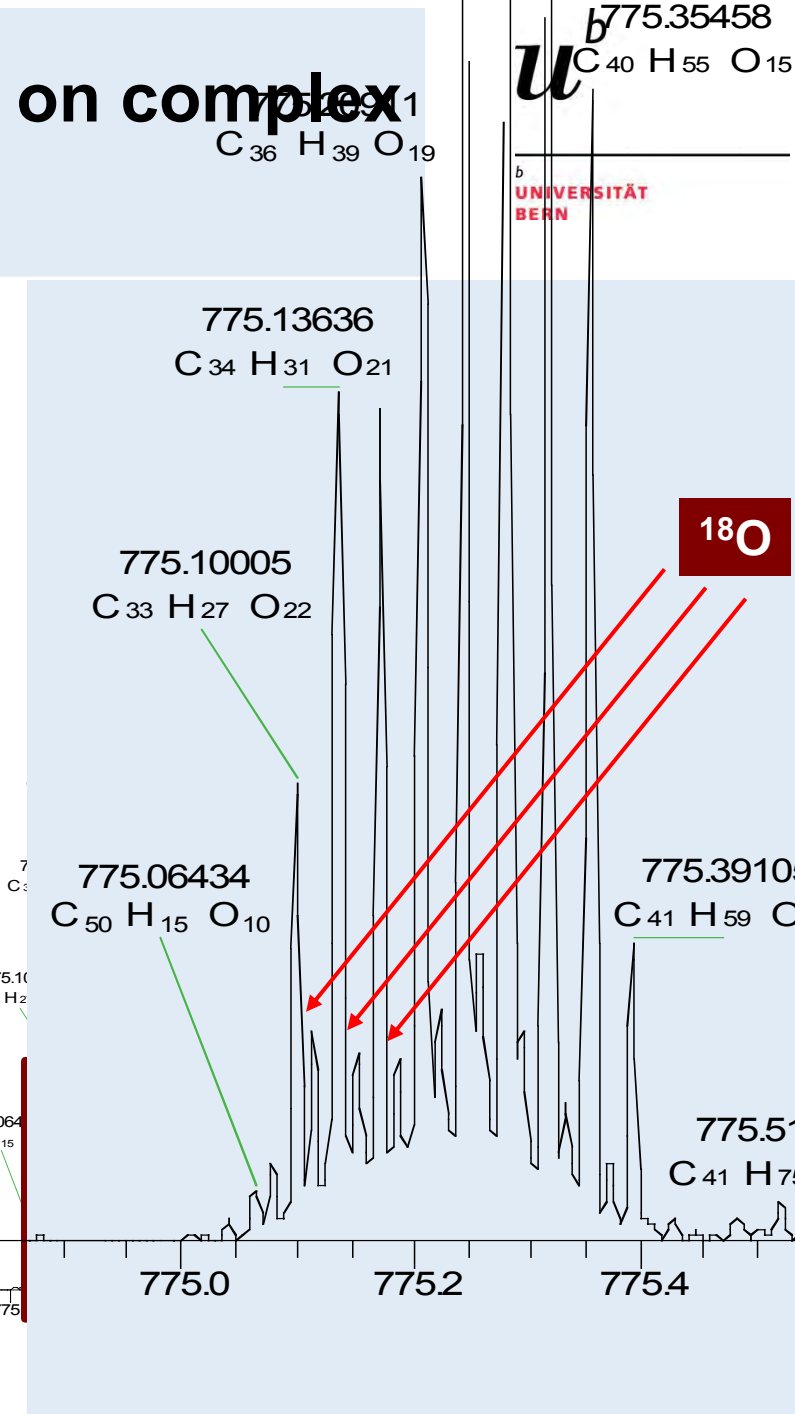
fulique pos SIM700-800FT #6-336 RT: 0.15-9.77 AV: 331 NL: 5.08E3
T: FTMS + pESI SIMms [700.00-800.00]



^{13}C



^{18}O



u^b

b
UNIVERSITÄT
BERN